scientific reports

Check for updates

OPEN

Enhancing the mechanical and shear behavior of clay soil using lime, Nano-MgO, and recycled PET fibers: experimental and UPV-based assessment

Ali Akbar Amiri[1], Nima Ranjbar Malidarreh[2]✉, Saman Soleimani Kutanaei[1], Ali Seyedkazemi[1] & Abdullah Davoudi-Ki[1]

Clay soils, due to their inherent low strength and undesirable engineering properties, usually require improvement and stabilization before use in geotechnical projects. In this study, a hybrid improvement system including lime, nano-magnesium oxide (nano-MgO), and recycled polyethylene terephthalate (PET) fibers was examined as an integrated chemical–mechanical approach for improving clay soil behavior. For this purpose, unconfined compressive strength (UCS), indirect tensile strength (ITS), direct shear, and ultrasonic pulse velocity (UPV) tests were performed on samples with various additive contents at curing times of 7, 14, 28, and 90 days. The results showed that the optimum mixture containing 10% lime, 2% nano-MgO, and 0.9% PET fibers considerably enhanced the mechanical and shear characteristics of the soil. The UPV results showed a strong and consistent relationship with the mechanical properties of the stabilized soil. This strong correlation confirms the reliability of UPV as a rapid and fully non-destructive evaluation method. Overall, the combined use of lime, nano-MgO, and PET fibers proved to be an effective strategy for improving the strength, durability, and structural integrity of clayey soils.

Keywords Stabilized clay soil, Ultrasonic pulse velocity, Nano-magnesium oxide, Non-destructive test

In recent decades, the growing demand for engineering structures on problematic soils and the scarcity of suitable land have made soil improvement and reinforcement critical topics in geotechnical engineering[1–5]. Problematic soils, particularly high-plasticity clays, are prone to differential settlement, structural cracking, and slope instability due to their unfavorable response to moisture variations and loading. These characteristics make construction on such soils particularly challenging. Therefore, various methods have been developed for soil improvement; among which lime stabilization is one of the most widely used techniques[6–11].

However, lime production accounts for approximately 7–8% of global carbon dioxide emissions. For this reason, the need to find more sustainable solutions to mitigate the environmental impacts of this process is highlighted[12–18]. In response, researchers have explored innovative and environmentally friendly additives aimed at reducing ecological impacts while improving the performance of stabilized soils. One of these materials is nanomaterials[19–23]. As a nanomaterial, Nano-MgO, with a particle size of approximately 15–20 nm and a high specific surface area of about 130–150 m^2/g, exhibits a high surface energy, which enhances its chemical reactivity. This property enhanced reactivity accelerates pozzolanic reactions through rapid adsorption of Ca^{2+} and SiO_2 ions, ultimately leading to the formation of cementitious compounds such as magnesium silicate hydrate (M–S–H) gel and calcium–magnesium silicate hydrate (C–M–S–H) gel. These reaction products fill fine pores and strengthen interparticle bonds, thereby improving the compaction and integrity of the soil structure[24–27]. In addition, soil reinforcement with synthetic fibers such as polyethylene terephthalate (PET) has been recognized as an effective complementary technique for soil improvement. PET fibers, often produced from recycled materials, have high tensile strength and chemical stability. These materials can help enhance soil strength and stability by preventing crack propagation and distributing stresses in the soil matrix[28–31].

[1]Department of Civil Engineering, Am.C. Islamic Azad University, Amol, Iran. [2]Department of Civil Engineering, No.C. Islamic Azad University, Nour, Iran. ✉email: nima.ranjbar@iau.ac.ir

In recent decades, numerous studies have been conducted to enhance the mechanical behavior of fine-grained and clayey soils through the use of nanomaterials and synthetic fibers. In general, these studies indicates that the addition of nanomaterials, such as nano-MgO, nano-calcium carbonate, and nano-clay, significantly increase compressive strength, reduce permeability, and improve soil microstructure. However, a critical review of the literature reveals that most research have primarily focused on the effect of a single type of additive. In contrast, the combined and interactive effects of chemical and mechanical additives (such as the combination of nanomaterials and fibers) has received less attention.

The study by Chen et al.[23] on loess soil revealed that the addition of 2% nano-MgO increased the UCS by approximately 72% and reduced the plasticity index. However, further increases in nano-MgO content resulted in strength reduction due to particle agglomeration and microcrack formation. Similar trends were reported by Wang et al. (2023) for cement-stabilized expansive clay soil treated with nano-MgO. They observed that nano-MgO contents of up to 1% increased compressive strength by about 35% after 7 days and 42% after 28 days of curing. In contrast, at higher contents, strength decreased due to nanoparticle agglomeration and microcrack formation within the cementitious matrix. Although this study comprehensively investigated the mechanical behavior of the samples, it only used destructive tests and did not analyze the long-term microstructure of the stabilized materials.

In the field of nano-calcium carbonate, Kannan et al.[32] reported an approximately twofold increase in compressive strength and a significant reduction in permeability of fine-grained soils. They attributed these improvements to the gradual formation of C–S–H phases during extended curing periods. Similarly, Mollaei et al.[33] investigated the effect of nano-clay on the dynamic behavior of silty sand soil. Their results showed that partial replacement of cement with nano-clay increased the shear modulus and reduced the damping ratio. However, they acknowledged that the creep behavior and long-term behavior of such mixtures still require more detailed evaluation.

On the other hand, several studies have investigated the use of synthetic fibers for reinforcing clayey soils. Yarbaşı and Kalkan[28] demonstrated that incorporating PET fibers into clay soils significantly improved their resistance to freeze–thaw cycles. As a result, the soil behavior shifted from a brittle response to a more ductile and resilient performance. Similarly, Huang et al. (2024) reported that adding approximately 0.6% polyvinyl alcohol (PVA) fibers to cement-treated clay soil increased its compressive strength by about 20%. The flexural strength also increased by around 15%, leading to improved soil ductility.

In addition, Kheyri et al.[24] examined the synergistic effects of nano-MgO and glass fibers on enhancing the physical and mechanical properties of clayey soils. Their results indicated that the combination of 1% nano-MgO and 1.5% glass fibers increased the compressive strength by 178% and elastic modulus by 143%. ANOVA results confirmed the statistically significant effects of both additives and their interaction. The notable contribution of this study was the analytical approach employed to determine the contribution of each additive in improving mechanical parameters. However, the authors did not evaluate the microstructural characteristics or apply non-destructive testing methods, which represents an important gap in the existing literature.

From a chemical perspective, Yao et al.[34] showed that adding nano-MgO to cement-stabilized silty soil increased cohesion and the internal friction angle. The improvement was observed up to an optimal nano-MgO content of 1%, resulting in a denser soil structure. However, at higher contents, strength decreased due to microcrack formation. These observations are consistent with the findings reported by Wang et al.[26] and Huang et al.[34], highlighting the need to determine the optimal content of nanomaterial in multi-component mixtures. Table A1 (Appendix) summarizes the key findings and limitations of previous studies, which helped identify the research gaps addressed in this work.

A systematic review of previous studies indicates that most research has focused on the effects of individual additives, such as lime, nanomaterials, or synthetic fibers, on soil behavior. In contrast, the combined use of these materials has received far less attention. Consequently, the synergistic interaction between chemical stabilizers (e.g., lime and nano-MgO) and mechanical reinforcements (e.g., PET fibers) remains insufficiently understood. In addition, non-destructive techniques have rarely been used to evaluate the mechanical performance and microstructural development of stabilized soils. These methods can provide valuable insight into strength evolution over time. Moreover, lime production contributes significantly to global CO_2 emissions. This highlights the need for more sustainable alternatives, such as nano-MgO and recycled PET fibers. Together, these limitations highlight the need for an integrated research approach. This approach should simultaneously examine the mechanical response and microstructural behavior of clayey soils treated with environmentally sustainable additives.

In this study, the combined effect of lime, nano-MgO, and PET on the mechanical and shear behavior of clay soil was investigated at curing times of up to 90 days. For this purpose, a series of destructive tests, including standard Proctor compaction, UCS, ITS, and direct shear, along with a nondestructive UPV test, were conducted. The use of this combination not only reduces lime consumption and thus greenhouse gas emissions but also helps reduce plastic pollution by utilizing recycled PET fibers. This study aims to provide a sustainable and practical solution to improve the behavior of unstabilized clay soil. Furthermore, this research aims to gain a deeper understanding of the interaction mechanism between nanomaterials and recycled fibers within the soil matrix.

Testing program

Materials

The soil used in this study was classified as high-plasticity clay (CH) according to the Unified Soil Classification System (USCS). Its physical and mechanical properties are summarized in Table 1. Figure 1 shows the grain-size distribution curve of the clayey soil used in this study.

USCS (ASTM D2487)	Gs (ASTM D854)	Atterberg limits (%) (ASTM D4318)			Compaction study (ASTM D698)		Free swell index (ASTM D4546)
		LL	PL	PI	MDD (kN/m^3)	OMC (%)	FSI (%)
CH	2.68	58	23	35	16.47	22.10	5.7

Table 1. Basic physical characteristics of the soil used in the experiments. Note: MDD: Maximum dry density, OMC: Optimum moisture content, Gs: Specific gravity.

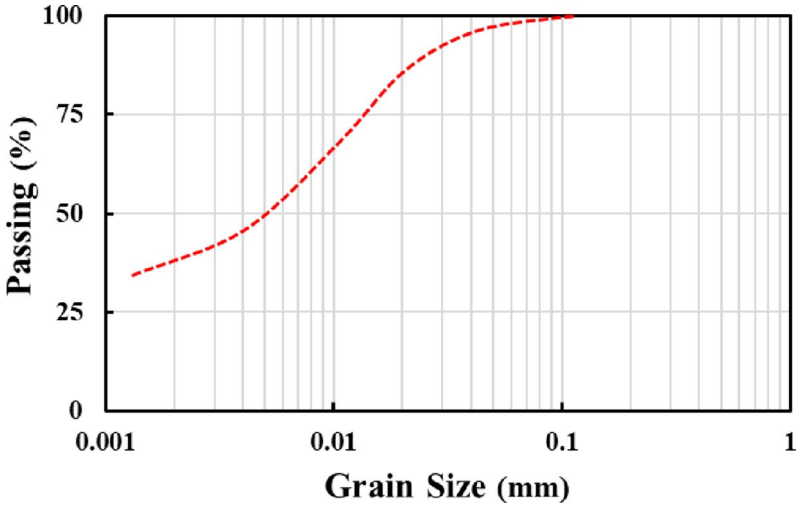

Fig. 1. Particle size distribution curve of the high-plasticity clay used in this study.

Chemical component	Al_2O_3	CaO	SO_2	Fe_2O_3	SiO_2	MgO	LOI	specific gravity (Gs)
Value (%)	0.76	73.5	0.12	0.16	1.5	0.50	23.46	2.3

Table 2. Chemical composition of lime. Note: Loss on Ignition: LOI, Gs: Specific gravity.

Properties	Value
Particle Size (nm)	15–20
Boiling point (˚C)	3600
Specific surface area (m^2/g)	130–150
Density (g/cm^3)	3.58
Purity (%)	99.5
Shape	Spherical

Table 3. Characteristics of nano-MgO.

To improve soil stabilization, hydrated lime ($Ca(OH)_2$) and nano-magnesium oxide (nano-MgO) were used as additives. Lime was incorporated at 0%, 4%, 6%, 8%, 10%, and 12% by dry weight of soil, while nano-MgO was added at 0%, 1%, 2%, 3%, and 4% by weight of lime. In addition, polyethylene terephthalate (PET) fibers were used as a reinforcing material at contents of 0%, 0.3%, 0.6%, 0.9%, and 1.2% by dry weight of soil.

The chemical composition of lime, the physical properties of nano-MgO, and the characteristics of PET fibers are provided in Tables 2 and 3, and 4, respectively.

Sample preparation

The clayey soil was sampled at a depth of approximately 1 m below the ground surface to minimize the influence of organic matter. The selected depth ensured that the soil was free from plant roots and vegetation; therefore, undisturbed (virgin) soil was used for specimen preparation. The collected soil was oven-dried at 105 ± 5 °C until a constant mass was achieved in accordance with ASTM D2216.

Properties	Values
Specific gravity(g/cm^3)	1.29
Color	White
Melting point (°C)	255
Diameter (mm)	0.1
Length (mm)	12
Moisture Content (%)	0.4

Table 4. PET fiber properties.

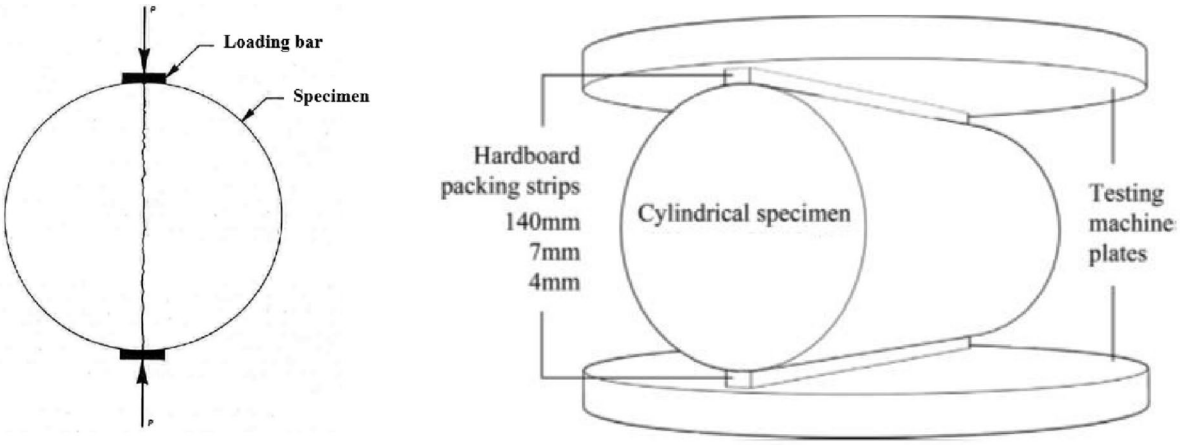

Fig. 2. ITS test setup: (**a**) diametral loading of the cylindrical specimen, and (**b**) specimen positioned between loading strips and testing machine plates.

The dried soil was then mixed with different lime contents (0%, 4%, 6%, 8%, 10%, and 12% by dry weight of soil). Nano-MgO was added at contents ranging from 0% to 4% by weight of lime, and polyethylene terephthalate (PET) fibers were incorporated at contents of 0% to 1.2% by dry weight of soil.

Then, water was gradually added to the dry mixture according to the optimum moisture content (OMC) obtained from the standard Proctor compaction test. The mixture was thoroughly blended to achieve a uniform and homogeneous structure.

For the UCS test, samples were prepared in a cylindrical form with a diameter of 52 mm and a height of 104 mm in five layers. The surface of each layer was lightly scratched before placing the subsequent layer to ensure proper bonding. Additionally, for the ITS test, specimens with a diameter of 50 mm and a height of 75 mm were prepared in five layers using the same compaction procedure as the UCS samples. In addition, for the direct shear test, samples with dimensions of $60 \times 60 \times 20$ mm were compacted in three layers.

After preparation, all samples were sealed in two plastic bags and cured for 7, 14, 28, and 90 days. All tests were performed under controlled laboratory conditions at 22 ± 2 °C.

For each mix design, three specimens were tested, and the average results exhibited standard deviations in the range of 3–5%.

Tests

To accurately evaluate the mechanical and structural properties of the stabilized samples, a comprehensive testing program carried out according to the relevant standards. The UCS test was conducted according to the ASTM D2166 at a strain rate of 1.2 mm/min. Additionally, the ITS test was performed following ASTM D3967. In this test, cylindrical specimens were positioned horizontally between two loading strips, and a compressive load was applied along the diametral axis using a uniaxial loading device (Fig. 2). This loading configuration induces tensile stresses perpendicular to the applied load, resulting in tensile failure at the center of the specimen.

The non-destructive UPV test was conducted according to ASTM D2845 to assess the internal uniformity and integrity of the samples. Ultrasonic waves with a frequency of 54 kHz were transmitted through the sample, and the wave travel time was recorded. This method is particularly effective for detecting internal defects, such as voids or microcracks, which can significantly influence soil mechanical behavior.

Direct shear tests were carried out in accordance with ASTM D3080 to determine the parameters of the drained shear strength of soil, including cohesion (c) and internal friction angle (φ). In this test, the samples were subjected to normal stresses of 75, 150, and 350 kPa. These parameters are essential for evaluating the bearing capacity and lateral earth pressure in geotechnical design. In addition, the direct shear test provides plane strain conditions that are closer to field behavior, making it a suitable method for investigating soil shear response under practical loading conditions.

Results and discussion

Standard proctor compaction

In this section, different lime contents ranging from 0% to 12% by dry weight of soil (in 2% increments) were first added to the samples to evaluate their effects on the optimum moisture content (OMC) and maximum dry density (MDD). Subsequently, a portion of the lime was replaced with nano-MgO. For this purpose, nano-MgO was added at 0%, 1%, 2%, 3%, and 4% by weight of lime, and its influence on soil compaction characteristics was examined.

Figure 3 illustrates the effect of lime content on MDD and OMC. As the lime content increases, MDD decreases while OMC increases.

Figure 3 shows that as the lime content increases from 0% to 12%, the MDD decreases by approximately 11%. This reduction results from a combination of physical and physicochemical mechanisms.

From a physical standpoint, the specific gravity of lime (≈ 2.30) is lower than that of the soil particles (≈ 2.68); therefore, increasing lime content reduces the overall unit weight of the mixture. In addition, lime reactions promote cation exchange and reduce the thickness of the diffuse double layer. This process leads to flocculation of clay particles and an increase in interparticle voids. As a result, part of the compaction energy is consumed in rearranging aggregated particles rather than increasing density. This combined physical–chemical behavior is consistent with the well-established mechanisms of lime–clay interaction reported in the literature.

As shown in Fig. 3, the OMC of high-plasticity clayey soil stabilized with 12% lime increased by approximately 28% compared with unstabilized soil. This increase is mainly attributed to the higher water demand required to activate the chemical reactions between lime and the clay minerals. The relatively larger increase in OMC observed in this study, compared with some previous studies, can be attributed to the high plasticity of the soil. High-plasticity clays typically possess a larger reactive surface area. As a result, a higher amount of water is required to facilitate lime-induced reactions.

Shirvani and Noorzad[35] investigated the effect of adding wood sludge ash with high CaO content on the compaction characteristics of clayey soils. They reported that adding 7% of this ash reduced the MDD by up to 7% and increased the OMC by 23%. Similarly, Noorzad and Motevalian[36] reported that the addition of lime led to a decrease in MDD and an increase in OMC in clayey soils. The trend observed in the present study is consistent with these findings. This agreement confirms that lime primarily modifies soil structure by promoting particle aggregation and increasing the water demand required for chemical activation. The higher OMC also reflects the increased lubrication requirement of flocculated clay aggregates, which need additional water to allow effective particle rearrangement during compaction.

Following this, the effect of different contents of nano-MgO on the compaction behavior of lime-treated soils was examined. The changes in MDD and OMC were analyzed to better understand the combined influence of lime and nano-MgO on the compaction characteristics. Figures 4 and 5 present the variations in MDD and OMC, respectively, for CH clay stabilized with 4%, 6%, and 8% lime at different nano-MgO contents.

Figures 4 and 5 show that increasing the nano-MgO content in lime-stabilized CH clay leads to a decrease in MDD and an increase in OMC. For samples stabilized with 4%, 6%, and 8% lime, the addition of 4% nano-MgO reduced the MDD by approximately 11.2%, 14.6%, and 15.6%, respectively. Meanwhile, the OMC increased by about 21.8%, 28.6%, and 32.8% compared with the corresponding lime-treated samples without nano-MgO. Although these changes are evident, they indicate a secondary influence of nano-MgO on the compaction characteristics relative to the dominant effect of lime content.

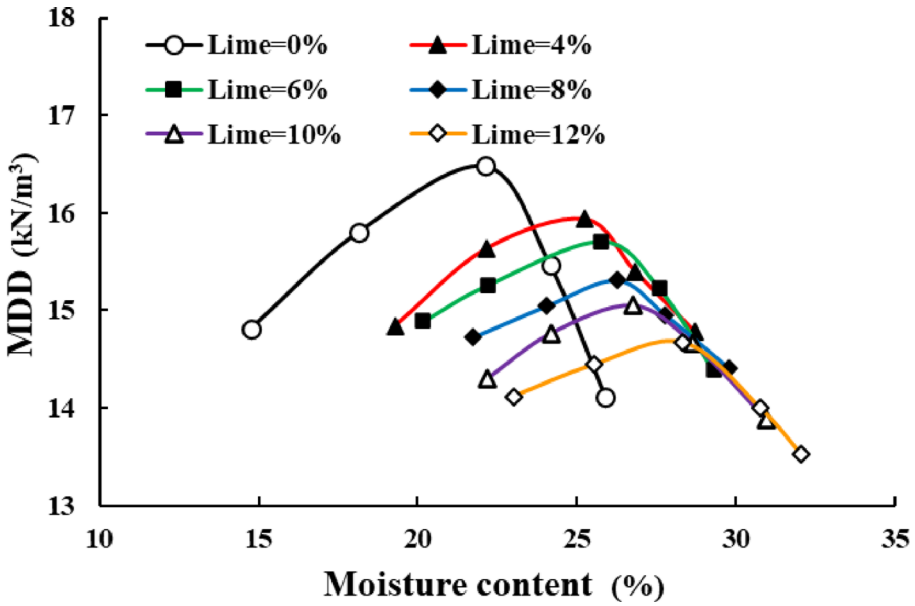

Fig. 3. Compaction curves of high-plasticity (CH) clay at different lime contents.

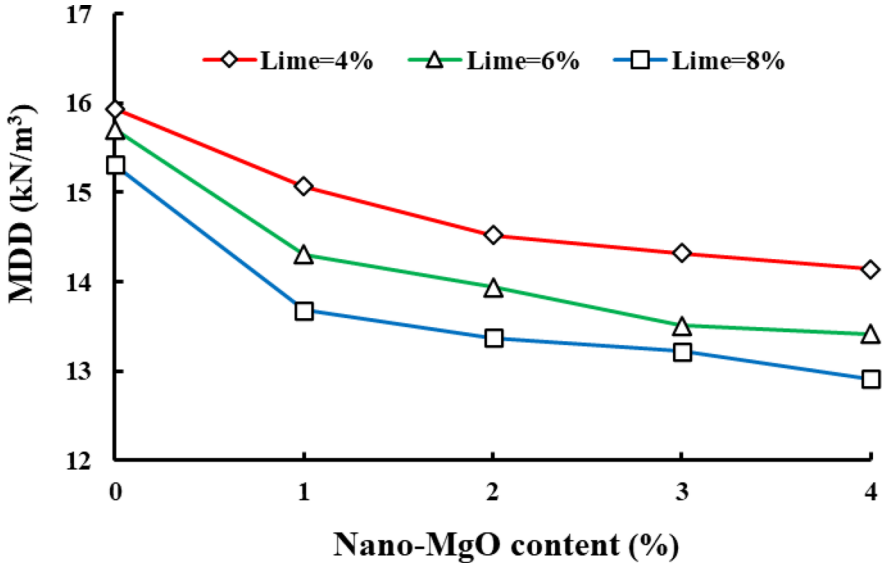

Fig. 4. Variation of maximum dry density (MDD) with nano-MgO content for CH clay stabilized with 4%, 6%, and 8% lime.

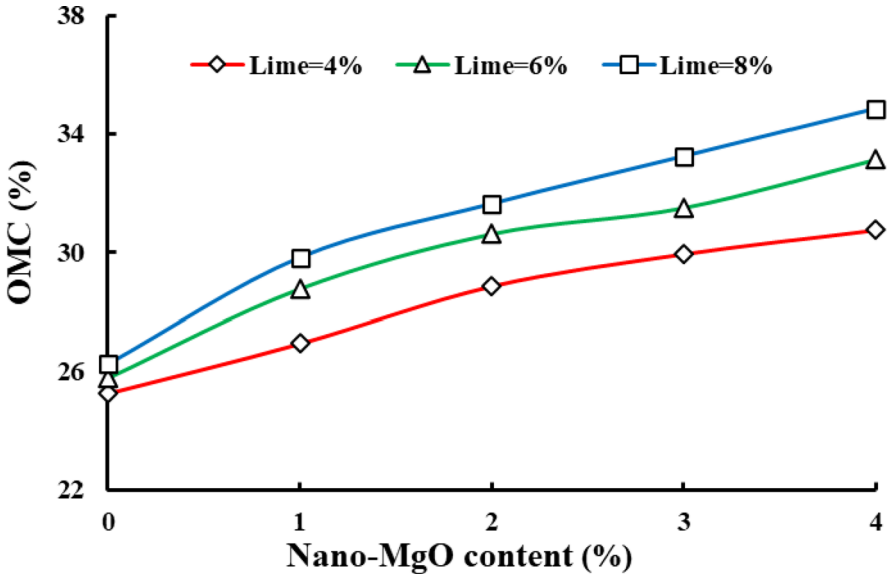

Fig. 5. Variation of optimum moisture content (OMC) with nano-MgO content for CH clay stabilized with 4%, 6%, and 8% lime.

The observed trends can be attributed to the high reactivity and large specific surface area of nano-MgO, which enhance pozzolanic reactions and slightly modify the early soil fabric. The formation of M–S–H and C–S–H gels (Chen et al., 2023; Kheyri et al., 2025) alters particle bonding and increases water demand. As a result, the increase in OMC mainly reflects the strong surface adsorption capacity of nano-MgO. It also indicates the formation of a more aggregated soil structure, which requires additional water for lubrication and particle rearrangement[25].

Similar observations have been reported in previous studies on various nanomaterials. For example, nano-calcium carbonate increased OMC and reduced MDD in clayey soils[37], while nano-silica produced a comparable response in sandy soils[38]. In cement-stabilized CL soil, nano-Al_2O_3 was also shown to increase OMC and reduce dry density[12].

Studies on nano-MgO report similar trends, with increased water retention and reduced dry density at low contents due to enhanced surface adsorption. At higher dosages, particle clustering occurs, which reduces compaction efficiency[25]. In addition, nano-MgO accelerates the formation of C–S–H and M–S–H gels, modifying soil microstructure and improving particle bonding while limiting achievable dry density[24].

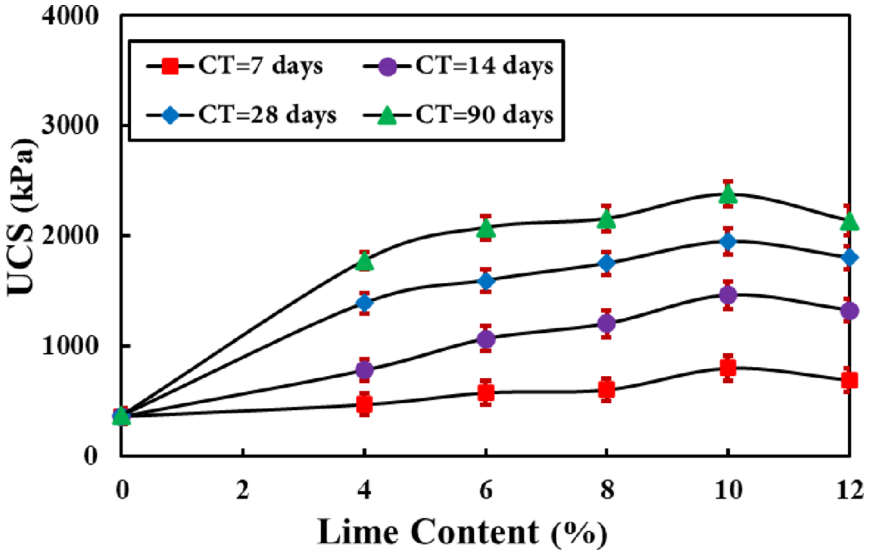

Fig. 6. Unconfined compressive strength (UCS) of lime-stabilized CH clay at different lime contents and curing times (7, 14, 28, and 90 days).

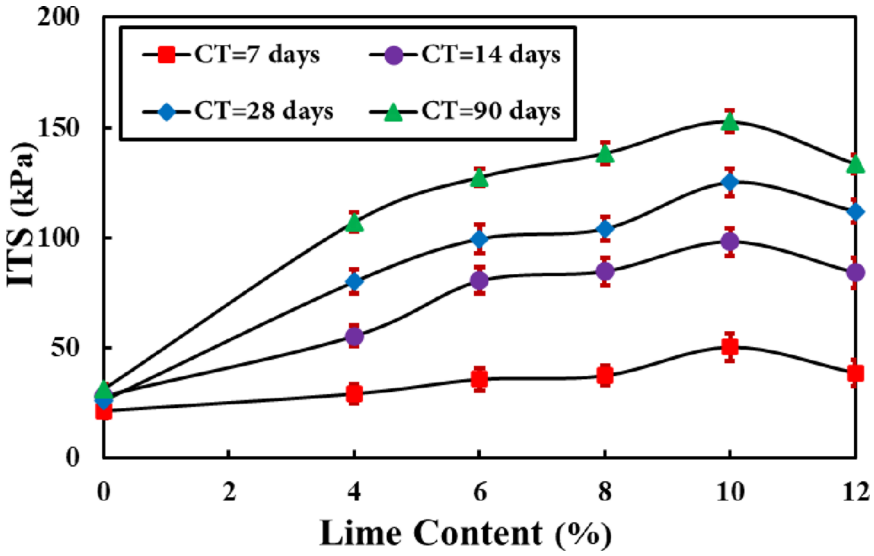

Fig. 7. Indirect tensile strength (ITS) of lime-stabilized CH clay at different lime contents and curing times (7, 14, 28, and 90 days).

These comparisons indicate that different nanomaterials vary in reactivity. However, common mechanisms such as surface adsorption, early gel formation, and microstructural rearrangement consistently lead to higher OMC and lower MDD. The results of the present study follow this established trend; however, the magnitude of the observed response suggests a stronger influence of nano-MgO, which can be attributed to its higher chemical reactivity.

Unconfined compressive strength and indirect tensile strength tests

This section presents the results of UCS and ITS tests conducted on clayey soil stabilized with lime and nano-MgO. This analysis aims to evaluate the effect of different combinations of these materials, along with curing time, on the mechanical properties of the soil.

In addition, the optimum composition for use in construction and soil improvement projects is determined. Figures 6 and 7 illustrate the variations in UCS and ITS of clayey soil at curing times of 7, 14, 28 and 90 days for different lime contents.

As illustrated in Figs. 6 and 7, increasing the lime content up to 10% led to a noticeable enhancement in both UCS and ITS values. Specifically, after 28 days of curing, the UCS and ITS of the samples treated with 10% lime increased by approximately 359% and 381%, respectively, compared to the untreated soil. This strength

gain mainly results from hydration and pozzolanic reactions between lime and clay minerals. In the early stage, lime hydrates to form calcium hydroxide, which then reacts with the silica and alumina present in the clay and produces C–S–H and C–A–H gels. These reaction products gradually fill voids and strengthen the bonds between particles. As a result, the soil structure becomes denser, which is consistent with the well-documented behavior of lime-stabilized clays. One of the key contributors to this improvement is the formation of C–S–H gel. **This gel has an exceptionally large specific surface area (approximately 100–700 m^2/g)** and consists of fine particles in the range of **5–25 nm.** The spacing between these particles is on the order of eighteen angstroms, which results in stronger van der Waals forces compared with the larger crystals of $Ca(OH)_2$. This very fine microstructure leads to tighter bonding among soil particles and plays an important role in the significant increases observed in UCS and ITS.

Curing time has an important effect on the reactions of lime with clay. The UCS of clayey soil stabilized with 10% lime increased by 82%, 142%, and 196% as the curing time was increased from 7 to 14, 28, and 90 days, respectively. The steeper increase in strength during the early curing period (7–28 days) reflects rapid pozzolanic activity. In contrast, the slower increase observed from 28 to 90 days corresponds to the gradual formation and maturation of long-term hydration products. This time-dependent pattern is typical for lime-stabilized soils, which generally show fast initial strength gains followed by more gradual improvements in stiffness and tensile resistance.

Furthermore, when the lime content exceeded 10%, a reduction in strength was observed. For instance, the UCS and ITS of the samples treated with 12% lime decreased by approximately 10% and 12.5%, respectively, compared to the samples stabilized with 10% lime. This reduction at lime contents above the optimum occurs because the soil becomes saturated with calcium hydroxide once the reactive **capacity** is exceeded. The excessive formation of calcium hydroxide in the soil leads to the development of **large and weak prismatic crystals** that cannot form strong bonds with soil particles. **These crystals increase soil porosity and weaken the gel bonds formed by C–S–H and C–A–H**. For this reason, increasing lime content more than the optimum content decreases the number of effective bonds, leading to a reduction in UCS and ITS. These reductions are attributed to the diminished contribution of pozzolanic products relative to the presence of excess $Ca(OH)_2$.

Figures 8 and 9 illustrate the variations in UCS and ITS with different nano-MgO replacement ratios for clayey soil containing the optimum lime content after curing periods of 7, 14, 28, and 90 days.

Figures 8 and 9 show that increasing the nano-MgO content up to a replacement ratio of 2% led to an increase in both UCS and ITS. The UCS and ITS of samples containing 10% lime with a 2% nano-MgO replacement ratio increased by approximately42.5% and 60%, respectively, after a curing time of 90 days. This improvement can be attributed to the enhanced reactivity introduced by nano-MgO, which accelerates the early pozzolanic reactions and strengthens the soil structure more effectively than lime alone.

In mixtures containing both lime and nano-MgO, calcium hydroxide reacts with silica and alumina to form C–S–H and C–A–H, while magnesium hydroxide reacts mainly with silica to produce M–S–H. Additional phases such as magnesium–calcium hydrates (M–C–H) and magnesium–aluminum layered double hydroxides (Mg–Al–LDH) may also form. The development of these products results in a denser matrix and stronger interparticle bonding, particularly at longer curing ages. As reported by Chen et al.[25] and Kheyri et al.[24], nano-MgO accelerates the transformation of $Mg(OH)_2$ into M–S–H, improves particle interlocking, and reduces porosity.

The optimum nano-MgO replacement ratio was approximately 2% by the weight of lime. At this level, nano-MgO is well dispersed and actively participates in cementitious reactions. However, higher contents cause particle agglomeration and excess $Mg(OH)_2$ formation, which forms weak crystals with limited bonding ability.

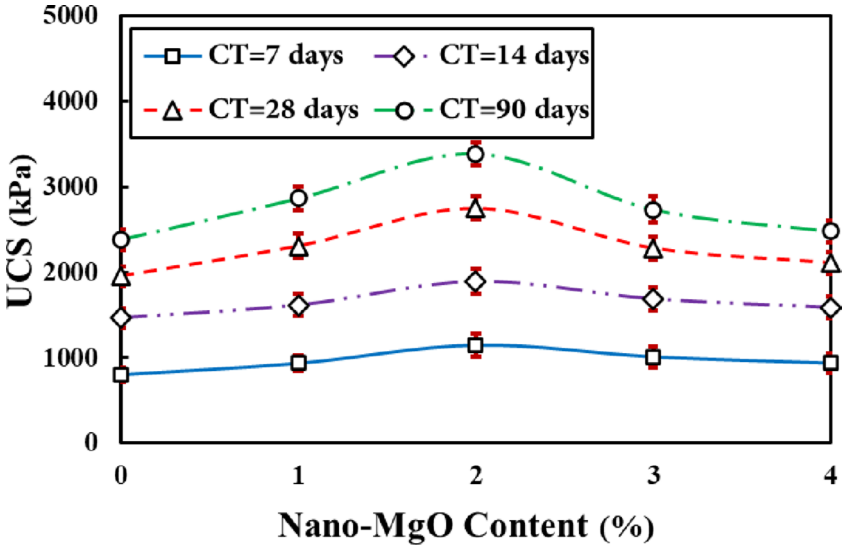

Fig. 8. Effect of lime replacement with nano-MgO on the UCS of CH clay containing the optimum lime content at curing times of 7, 14, 28, and 90 days.

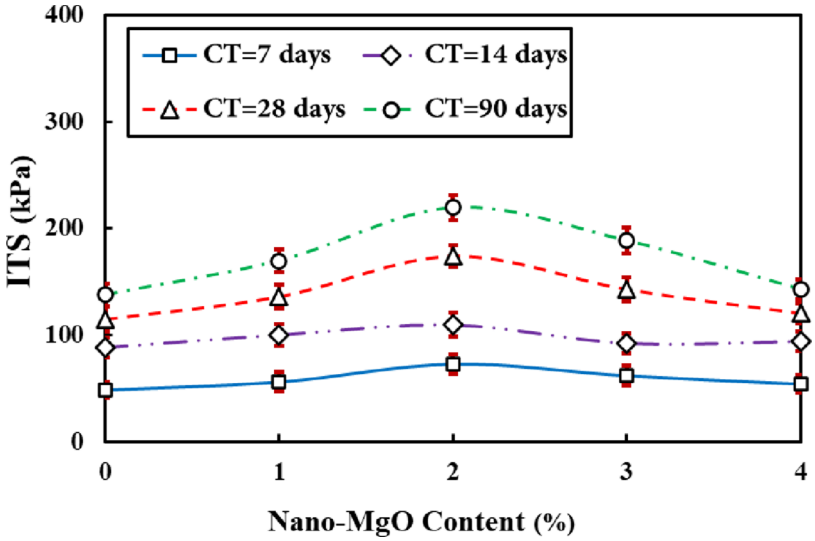

Fig. 9. Effect of lime replacement with nano-MgO on the ITS of CH clay containing the optimum lime content at curing times of 7, 14, 28, and 90 days.

These agglomerated areas can act as weak points in the matrix and may initiate microcracks, ultimately reducing strength. After 90 days of curing, UCS and ITS at a 4% replacement ratio decreased by 26% and 34%, respectively, compared with the optimum value, consistent with the observations reported by Chen et al.[24].

Previous studies have consistently shown that nanomaterials can improve soil strength by enhancing gel formation and modifying microstructure. Improvements in UCS ranging from about 30% to more than 100% have been reported for soils treated with nano-silica, nano-calcium carbonate, nano-aluminum oxide, nano-iron oxide, and nano-bentonite[39–42]. These findings are consistent with the present study and confirm the positive influence of nano-MgO on soil stabilization. Overall, previous research supports the conclusion that nano-MgO provides an effective pathway for improving the mechanical behavior of fine-grained soils.

Figures 8 and 9 further show that UCS increased by 65%, 140%, and 195% as the curing time increased from 7 to 14, 28, and 90 days. The early-age increases reflect rapid gel formation and initial bonding, while the longer-term gains result from the continued development of C–S–H, C–A–H, and M–S–H phases. Over time, this leads to a more coherent internal network that reduces porosity and limits particle displacement under loading. These time-dependent effects are consistent with earlier studies[39,40], all of which reported meaningful increases in UCS with extended curing durations.

In this section, the effect of adding PET fibers on the mechanical performance of clayey soil stabilized with 10% lime and replacing 2% lime with nano-MgO is investigated. Figures 10 and 11 show the changes in UCS and ITS at different curing times and with different PET fiber contents.

Figures 10 and 11 exhibit that increasing the PET fiber content led to a noticeable improvement in both UCS and ITS. The UCS and ITS in the sample stabilized with 10% lime containing 2% nano-MgO and reinforced with 0.9% PET fibers increased by 22.5% and 41%, respectively, after 28 days of curing.

This improvement in strength is mainly due to the reinforcing role of PET fibers, which create a three-dimensional network within the stabilized soil and act as flexible bridges linking soil particles and hydration products[34]. This network redistributes stresses, delays crack initiation, and controls the growth of developing cracks, resulting in higher deformation resistance and a more ductile failure response. The greater increase in ITS compared with UCS confirms that PET fibers are particularly effective in enhancing tensile load resistance and crack-bridging capacity. At the optimum content of 0.9%, the fibers are well dispersed and efficiently bridge microcracks, producing the highest strength. However, at higher dosages, fibers tend to cluster and disrupt uniform stress transfer, creating weak zones that explain the slight reduction in performance at 1.2% fiber content. These observations indicate that fiber effectiveness depends strongly on achieving uniform dispersion within the soil matrix.

The UCS of mixtures reinforced with 0.9% and 1.2% fibers was only about 2% and 2.6% higher than the lime–nano-MgO mixture without fibers, confirming that excessive fiber addition does not improve performance.

Previous studies on nano-stabilized and lime-treated soils have generally reported UCS improvements in the range of 30–110% compared with untreated conditions—for example, about 70% with 1% nano-silica, 41% with 1% nano-calcium carbonate, 49–109% with different nanomaterials, and up to 100% with nano-alumina. In contrast, the present results show a much greater enhancement: after 90 days of curing, UCS increased by approximately 544% with 10% lime, 814% with lime + 2% nano-MgO, and 892% when 0.9% PET fibers were also added. This substantial gain highlights the strong synergistic action between chemical stabilization (lime and nano-MgO) and mechanical reinforcement (PET fibers), where the combined effects of enhanced gel formation and fiber-bridging produce improvements that are far beyond what each additive can achieve on its own.

Furthermore, a correlation was established between the UCS and ITS results for PET fiber-reinforced and unreinforced samples stabilized with lime and nano-MgO. This relationship is provided for all fiber contents and

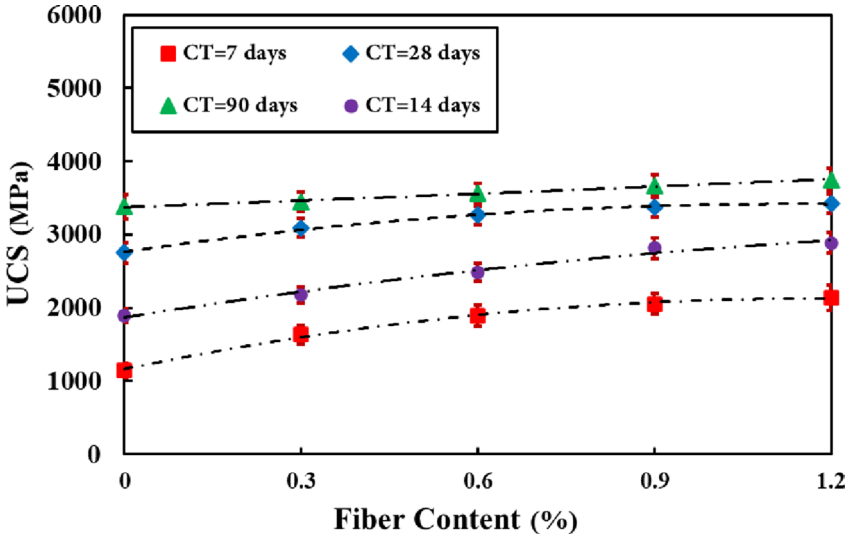

Fig. 10. Variation of UCS of CH clay stabilized with 10% lime and 2% nano-MgO replacement at different PET fiber contents and curing times.

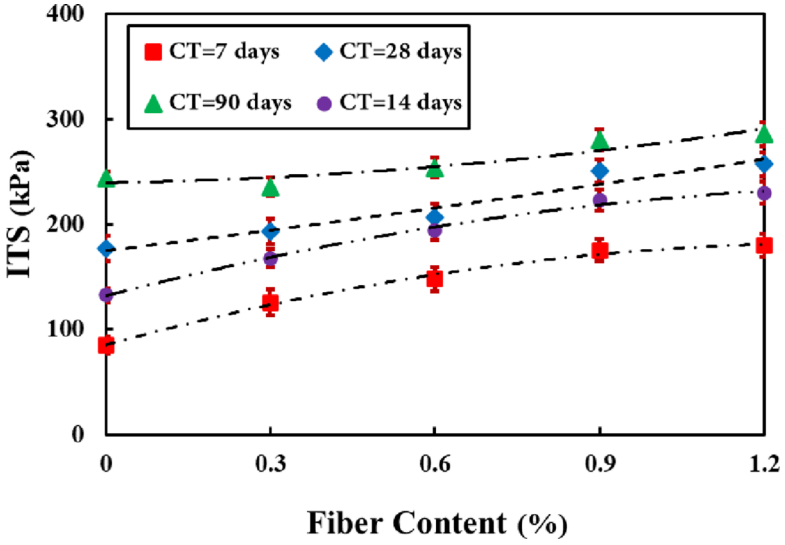

Fig. 11. Variation of ITS of CH clay stabilized with 10% lime and 2% nano-MgO replacement at different PET fiber contents and curing times.

different curing times. Figure 12 and Eqs. 1 and 2 show the variations in ITS based on UCS for unreinforced and PET fiber-reinforced samples, respectively.

$$ITS = 0.0247e^{0.792UCS} \quad (1)$$

$$ITS = 0.073e^{0.5071UCS} \quad (2)$$

In Eqs. (1) and (2), ITS denotes the indirect tensile strength (MPa), and UCS represents the unconfined compressive strength (MPa). The correlation coefficients (R^2) for Eqs. 1 and 2 are 0.87 and 0.97, respectively, indicating the high accuracy of these empirical relationships in estimating ITS. These results show that the proposed equations are satisfactory for predicting the ITS of stabilized samples. The higher R^2 value for PET-reinforced samples indicates that the addition of fibers creates a more uniform and predictable relationship between compressive and tensile behavior, due to enhanced crack-bridging and improved stress redistribution.

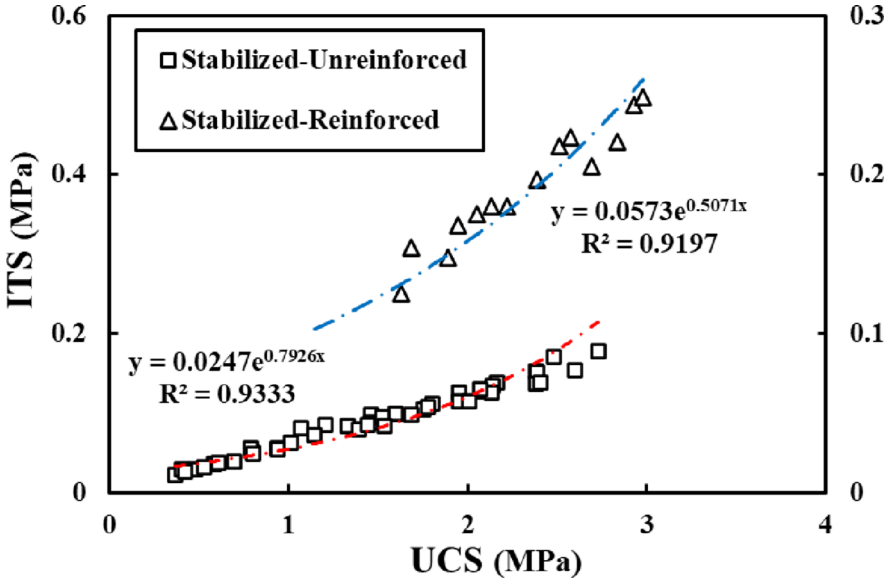

Fig. 12. Relationship between UCS and ITS for CH clay stabilized with lime, nano-MgO, and PET fibers at different curing times.

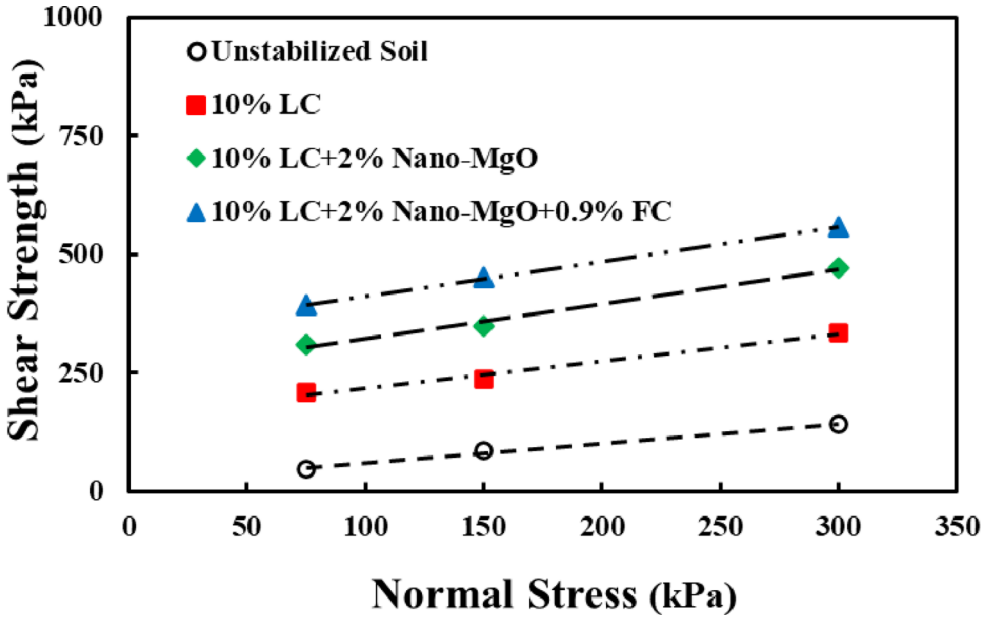

Fig. 13. Shear stress–normal stress relationship for stabilized CH clay after 28 days of curing (average of three tests).

Direct shear test

This section presents the results of stabilizing clayey soil with 10% lime, a combination of 10% lime and 2% nano-MgO replacement, and a similar sample reinforced with 0.9% PET fibers. Figures 13 and 14 show the variations in shear strength under different normal stresses for curing times of 28 and 90 days, respectively.

Figures 13 and 14 show that adding lime to CH clayey soil significantly improves its shear strength. At a lime content of 10%, the formation of C–S–H and C–A–H gels fills the pore spaces and creates a denser and more interlocked soil fabric, shifting the failure envelopes upward and to the right. This behavior reflects increases in both cohesion and frictional resistance. Such changes are consistent with the well-established mechanisms of lime stabilization. In this process, cementitious products bridge clay particles and enhance the overall integrity of the soil matrix.

Partially replacing lime with nano-MgO further strengthens the soil. Due to its high surface area and enhanced reactivity, nano-MgO accelerates pozzolanic reactions within the soil matrix. As a result, it promotes

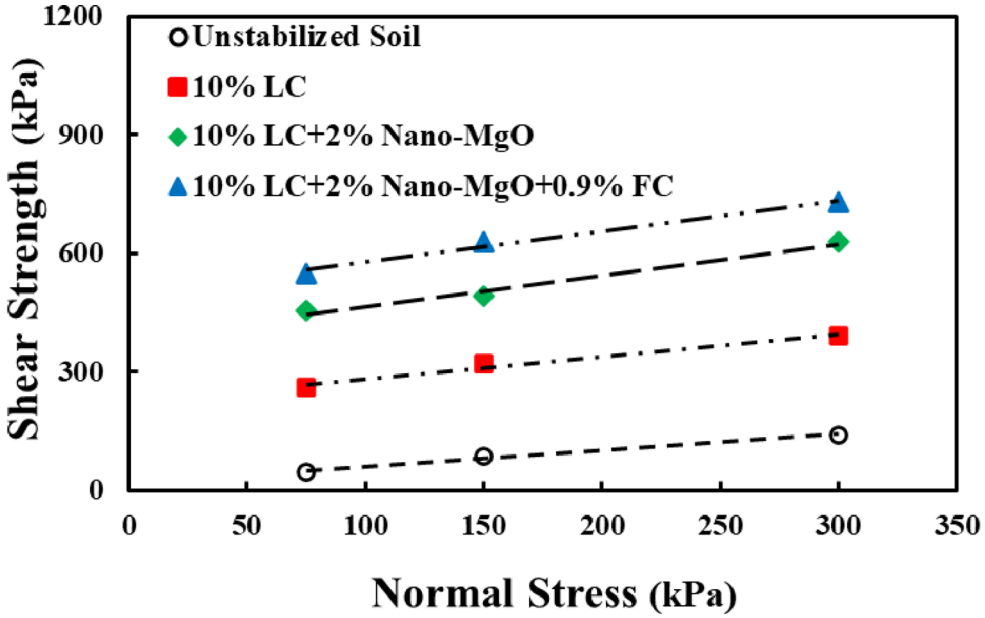

Fig. 14. Shear stress–normal stress relationship for stabilized CH clay after 90 days of curing (average of three tests).

the formation of additional cementitious products, particularly M–S–H, while also reducing microcracking. These changes contribute to a more continuous shear-resisting matrix and improve stress transfer across potential failure planes. The incorporation of PET fibers provides a complementary mechanical reinforcement mechanism. The fibers act as frictional–adhesive bridges that carry tensile stresses, delay the initiation and propagation of shear cracks, and contribute to a more ductile post-peak response. This combined chemical (nano-MgO) and mechanical (fiber) stabilization results in a further upward and rightward shift of the failure envelopes, indicating more effective mobilization of shear strength.

Curing time also plays a key role in the observed behavior. A comparison of the 28- and 90-day results indicates that extended curing allows pozzolanic reactions to proceed more completely.

As a result, larger amounts of C–S–H and M–S–H are formed over time. These compounds fill remaining voids, strengthen particle interlocking, and enhance the continuity of the soil matrix. Consequently, the shear strength increases over time due to both stronger chemical bonding and improved internal frictional resistance.

Cohesion and internal friction angle are among the most critical parameters affecting soil shear strength, as they significantly determine its mechanical behavior. These parameters are strongly influenced by the type of stabilizing materials used and the curing time. Accordingly, Figs. 15 and 16 present the variations in cohesion and internal friction angle for soils stabilized with 10% lime. The results are shown for samples containing 10% lime with 2% nano-MgO replacement, as well as similar samples reinforced with 0.9% PET fibers, at curing times of 28 and 90 days.

As observed in Fig. 15, adding 10% lime to the soil significantly increased cohesion, making it about 8.8 times higher than that of the unstabilized soil. This increase is attributed to the chemical reactions between lime and soil, which strengthen the structure and lead to the formation of cementitious products.

On the other hand, replacing 2% of the lime with nano-MgO further enhanced cohesion by up to 60% compared to the lime-only condition. The high reactivity of nano-MgO and its ability to accelerate pozzolanic processes play a key role in reinforcing and integrating the soil structure. Furthermore, the combination of 0.9% PET fibers with 10% lime and 2% nano-MgO resulted in the highest cohesion, increasing it by approximately 30%. The fibers act as reinforcing elements by forming a three-dimensional network within the soil matrix. This network reduces stress concentration at weak points, strengthens particle connections, and prevents soil separation and failure. As a result, this optimum combination leads to a significant improvement in cohesion and overall mechanical stability of the stabilized soil. The notable additional increase compared with lime alone highlights the higher early-stage reactivity of nano-MgO.

As shown in Fig. 16, the addition of stabilizing agents enhances the internal friction angle of the soil. The addition of 10% lime, a combination of 10% lime and 2% nano-MgO, and the same mixture with 0.9% PET fibers increased the internal friction angle by 30%, 47%, and 58%, respectively, compared to the unstabilized soil after 28 days of curing. Lime improves particle compaction and interlocking, while nano-MgO reduces void and increases cohesion, thereby enhancing resistance to sliding. Furthermore, PET fibers form a three-dimensional network within the soil matrix that strengthens interactions between particles. This network restricts their relative movement, leading to further improvements in the internal friction angle and overall shear strength. The increase in internal friction angle indicates that particle interlocking is enhanced not only through chemical bonding but also through mechanical reinforcement provided by the fibers.

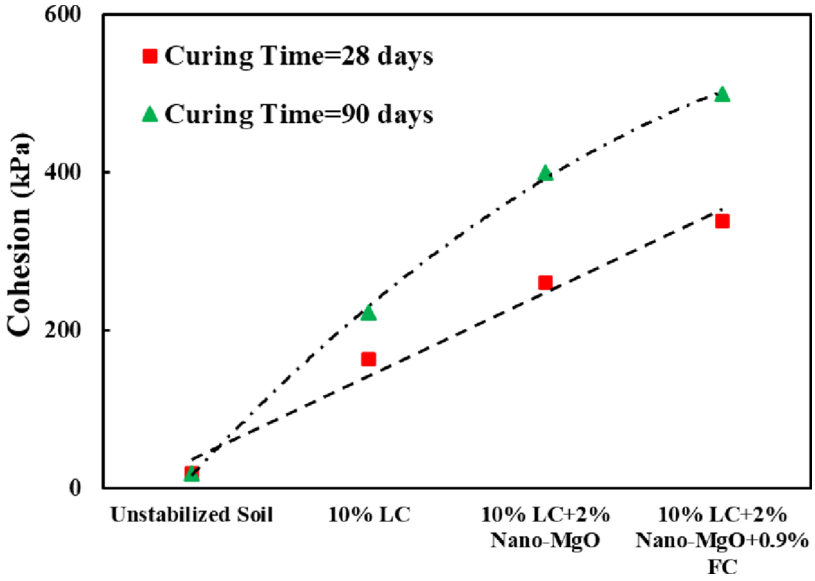

Fig. 15. Variation of cohesion (c) for CH clay stabilized with 10% lime, 2% nano-MgO replacement, and 0.9% PET fibers at different curing times.

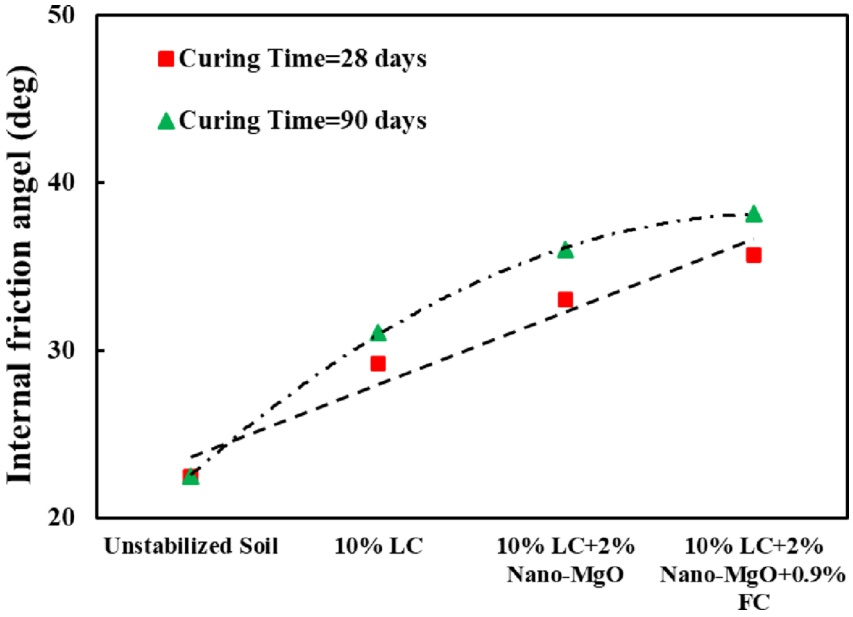

Fig. 16. Variation of internal friction angle (φ) for CH clay stabilized with 10% lime, 2% nano-MgO replacement, and 0.9% PET fibers at different curing times.

A comparison with previous studies shows that the improvements in cohesion and internal friction angle observed in this study follow a similar trend. In particular, the enhanced shear strength achieved using lime, nano-MgO, and PET fibers is consistent with findings reported in earlier research. For instance, Gu et al.[43] reported increases of approximately 45% in cohesion and 25% in the internal friction angle for clayey soil treated with 1% nano SiO_2. In the present study, replacing only 2% of the nano-MgO resulted in a 60% increase in cohesion compared with lime alone, highlighting the greater reactivity of MgO relative to SiO_2. Similarly, Buazar[44] reported a 3.07-fold increase in cohesion for nano silica-treated soils. However, in the present study, the combined use of lime, nano-MgO, and PET fibers resulted in a threefold increase in cohesion compared to lime-stabilized soil. This improvement corresponds to an approximately 8.8-fold increase relative to the untreated soil, exceeding the enhancements reported in most previous studies.

Moreover, the findings of Bagherzadeh Khalkhali et al.,[45] and Abisha et al.,[46] regarding increased cohesion and limited variation in the internal friction angle of soils stabilized with nanoclay are consistent with the behavior observed in the present study. However, the presence of PET fibers in the stabilizing composition

resulted in a much greater increase in the internal friction angle. Therefore, it can be concluded that the ternary composition of lime, nano-MgO, and PET fibers not only accelerates pozzolanic reactions, but also provides a coordinated increase in c and φ due to the formation of a three-dimensional reinforcing network; an effect that has not been reported with such magnitude in previous studies.

These microscopic mechanisms are further supported by the SEM observation of the stabilized and fiber-reinforced soil, as shown in Fig. 17. The SEM observations reveal that the fibers penetrate the soil matrix as long, randomly distributed filaments, connecting the particles in various orientations. This microstructural arrangement has led to the formation of a three-dimensional network within the soil structure, which binds fine clay particles and cementitious products to the fibers. The surface of the fibers was coated with layers of adhered particles and products of pozzolanic reactions, indicating the presence of a strong mechanical and chemical bonding between the fibers and the soil.

This effective bonding enhances stress transfer within the soil matrix, thereby improving its tensile and shear strength. The accumulation of stabilized soil and pozzolanic products around the fibers confirms that chemical reactions promote interlocking between soil particles and the filaments.

This interlocking mechanism enhances the structural integrity and overall stability of the treated soil sample.

From a geotechnical engineering perspective, this three-dimensional fiber-soil structure enhances volumetric cohesion, reduces stress concentration in weak areas, and improves the overall soil behavior. The fibers act as bridges between particles, preventing crack propagation; as a result, the toughness, ductility, and failure resistance of the stabilized soil are significantly increased.

The increase in curing time also has a significant effect on the shear strength parameters. As the curing period extends from 28 to 90 days, pozzolanic reactions become more complete, resulting in stronger chemical bonds between the soil particles and the stabilizing agents. Consequently, both cohesion and the internal friction angle increase across all samples. The cohesion and internal friction angle of the stabilized sample containing 10% lime, 2% nano-MgO, and 0.9% PET fibers increased by 47% and 7%, respectively, with increasing curing time. This trend highlights the progressive nature of pozzolanic bonding, particularly in systems incorporating both lime and nano-MgO.

In summary, lime plays the primary role in improving soil cohesion by initiating cementitious bonding. Nano-MgO further enhances this effect by promoting matrix densification and strengthening pozzolanic reactions. PET fibers complement the chemical stabilization by restricting particle movement and bridging potential failure planes. Together, these mechanisms produce a soil matrix with improved ductility, higher toughness, and enhanced long-term shear stability.

Ultrasonic pulse velocity

Figures 18 and 19 illustrate how the UPV changes with curing time in samples stabilized with different lime contents and varying replacement ratios of nano-MgO, measured at 7, 14, 28, and 90 days.

Figures 18 and 19 demonstrate that treating clayey soil with lime and nano-MgO leads to an increase in the UPV, indicating enhanced material integrity over time. The UPV increased by about 158% with the addition of 10% lime at a curing time of 90 days. Furthermore, with the addition of nano-MgO at a replacement ratio of 2% resulted in a further UPV increase of about 38% compared to the sample without nano-MgO. This improvement reflects the progressive densification of the soil matrix, as pozzolanic reactions promote the formation of a more continuous and rigid skeleton. As a result, ultrasonic waves propagate faster and with less scattering through

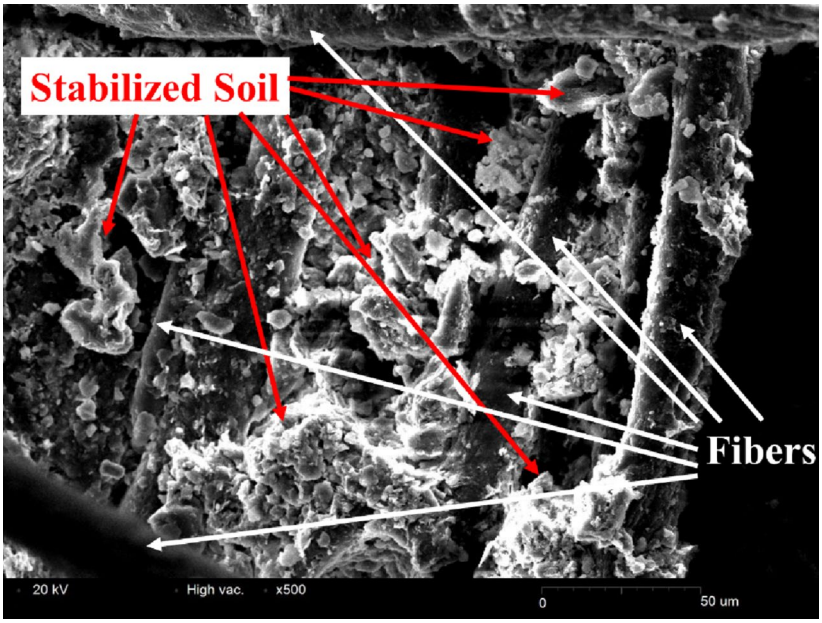

Fig. 17. SEM image showing the microstructural arrangement of the stabilized and fiber-reinforced CH clay.

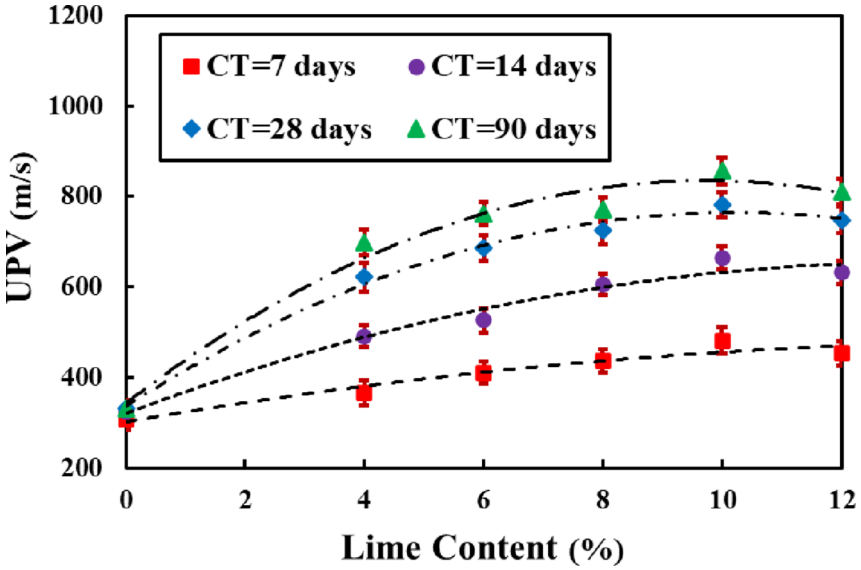

Fig. 18. Ultrasonic pulse velocity (UPV) variation with lime content at curing times of 7, 14, 28, and 90 days.

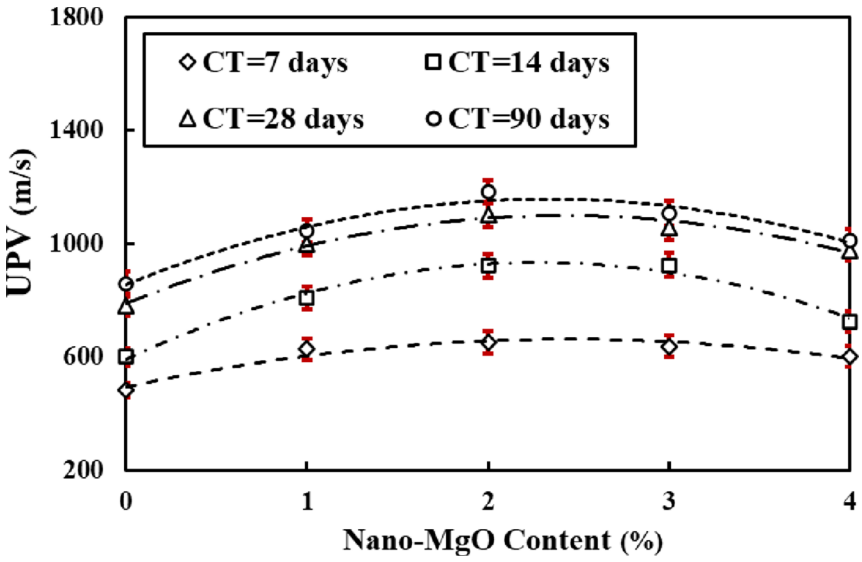

Fig. 19. UPV variation with nano-MgO replacement ratio for CH clay containing the optimum lime content at curing times of 7, 14, 28, and 90 days.

the stabilized soil, which is consistent with the known sensitivity of UPV to microstructural enhancement and reduced void continuity.

The enhancement in UPV is mainly attributed to improvements in the internal soil structure and changes in the wave propagation path. Pozzolanic reactions between lime and the clayey soil lead to the formation of stronger cementitious phases, which increase soil compaction and reduce interparticle voids. At the same time, the formation of C–S–H and M–S–H gels creates micro-scale bridges between adjacent particles, allowing ultrasonic waves to transfer energy more efficiently. Thus, the increase in UPV directly reflects the development of a stiffer and more continuous cemented soil skeleton.

Also, replacing lime with nano-MgO fills microscopic voids and accelerates pozzolanic reactions, creating a more homogeneous and stable structure. These structural changes lead to a more direct and shorter wave propagation path in the soil. The increased density, reduced void, and improved interparticle contact minimize wave reflection and energy loss. Thus, the waves travel through the soil more rapidly, showing the impact of lime and nano-MgO stabilization on wave transmission. According to Choobbasti et al.[27], incorporating 0.8% nano calcium carbonate into clayey soil resulted in a 15% increase in the UPV, reflecting improved material density and continuity.

However, as shown in Figs. 18 and 19, increasing the lime and nano-MgO content beyond the optimum level leads to a decrease in UPV. For example, the UPV of the sample containing 10% lime with a 4% nano-MgO replacement ratio decreased by approximately 14.4% compared to the optimum 2% nano-MgO replacement ratio after 90 days of curing. This reduction occurs because excessive amounts of lime or nano-MgO promote local agglomeration and the formation of coarse and weak $Mg(OH)_2$ and $Ca(OH)_2$ crystals, which interrupt the continuity of the soil skeleton. As a result, excess particles accumulate between soil grains, increasing porosity and creating structural discontinuities. In these conditions, ultrasound waves encounter more inhomogeneities in their path instead of passing directly and uniformly. Therefore, energy loss increases, and UPV decreases. Similarly, Kutanaei and Choobbasti[38] reported that the UPV of cement-stabilized soil decreased by 9% when the nano silica content increased from 8% to 12%.

Figure 20 shows the effect of adding PET fibers on the UPV of clayey soil stabilized with 10% lime containing a replacement ratio of 2% nano-MgO in terms of different PET fiber contents at different curing times.

As illustrated in Fig. 20, incorporating fibers led to a reduction in the UPV. Specifically, the UPV of clayey soil treated with 10% lime, where 2% was replaced by nano-MgO and reinforced with 0.9% PET fibers decreased by approximately 4.7% compared to the unreinforced sample. This reduction can be attributed to three main factors:

1. Horizontal orientation of PET fibers: During the compaction process, fibers generally align horizontally, perpendicular to the wave propagation path, causing wave reflection and refraction.
2. Creation of heterogeneity in the structure: The presence of fibers alters the microstructure of the sample, making it a non-homogeneous and dissipating part of the wave energy.
3. Flexibility of PET fibers: The lower elastic modulus of the fibers compared to soil and cementitious components reduces the stiffness of the wave propagation path, thereby decreasing UPV.

This indicates that fiber reinforcement, while beneficial for ductility, does not contribute to UPV because UPV primarily reflects stiffness rather than toughness.

Although the presence of fibers slightly decreases UPV, it does not imply structural weakness. In fact, the micro-gaps around fibers allow limited strain accommodation, which helps delay crack propagation under load. This explains why fiber-reinforced samples often show higher ductility despite a lower UPV value.

The UPV is a significant non-destructive index for evaluating the mechanical and geotechnical properties of materials, as it is strongly influenced by microstructure, internal compaction, and overall sample integrity. This parameter provides useful insight into changes induced by additives, compaction conditions, and environmental effects. These relationships were analyzed for both reinforced and unreinforced samples to clarify the influence of additives, particularly PET fibers, on mechanical performance. Such an analysis provides a useful basis for optimizing stabilized soils for engineering applications.

Figure 21 presents the relationship between UPV and both UCS and ITS for specimens with and without PET fiber reinforcement. The R^2 are 0.91 and 0.92, respectively, confirming the strong predictive capability of these empirical models in estimating UCS and ITS based on UPV measurements.

As illustrated in Fig. 22, exponential equations with R^2 of 0.8704 and 0.8064 for MDD and OMC indicate that UPV effectively predicts these variations. The use of exponential relationships reflects the nonlinear and complex behavior of these parameters, which are influenced by compressibility, porosity, and soil stiffness

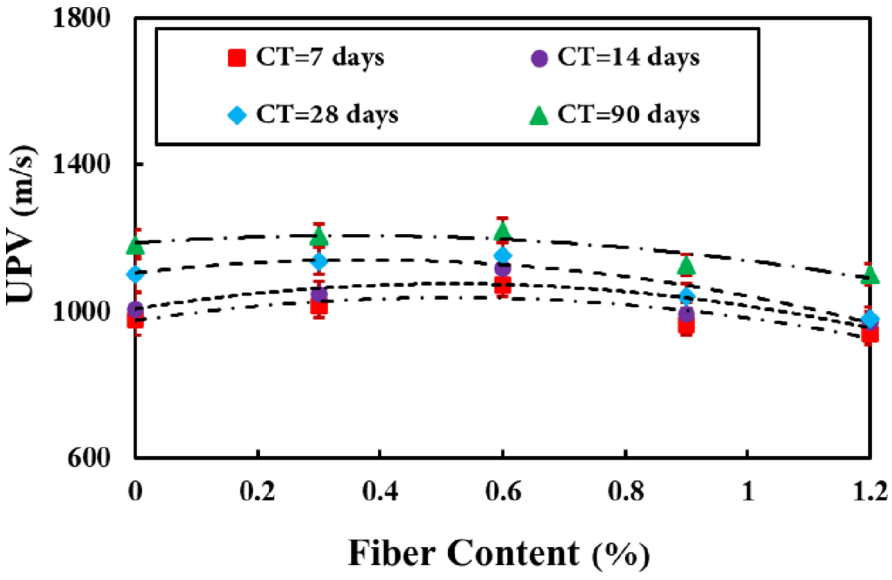

Fig. 20. UPV variation of CH clay stabilized with 10% lime and 2% nano-MgO replacement at different PET fiber contents and curing times.

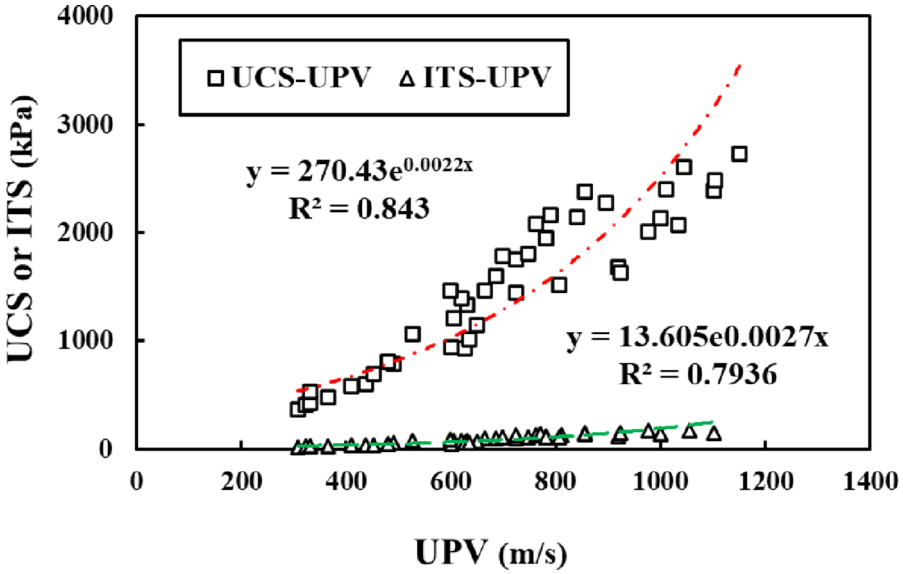

Fig. 21. Relationships among UCS, ITS, and UPV for CH clay at different lime contents, nano-MgO contents, and curing durations.

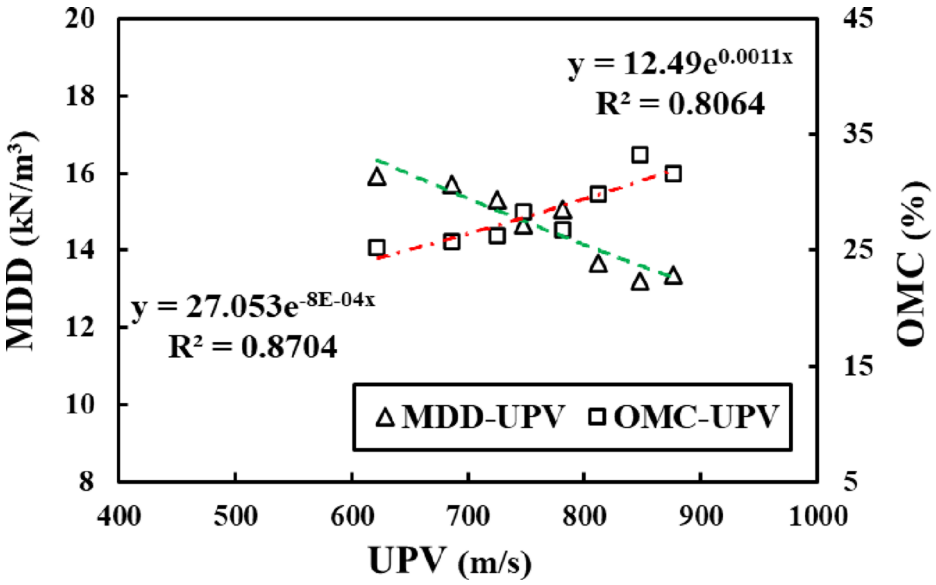

Fig. 22. Relationship between UPV and compaction parameters (MDD and OMC).

changes. This model highlights the significance of UPV as a dependable indicator for evaluating and forecasting the mechanical behavior of stabilized soils.

To extend the UPV-based prediction to shear strength components, Fig. 23 presents the correlations between UPV and the shear parameters (c and φ). Both parameters are exponentially related to UPV, indicating their nonlinear behavior. The internal friction angle shows an almost linear relationship with UPV, with a low slope and R^2=0.925. At the same time, cohesion shows an exponential relationship with R^2=0.7921, indicating a faster rate of change.

The overall trend shows that as UPV increases, the internal friction angle gradually increases, whereas cohesion is significantly more affected. The more significant impact on cohesion can be attributed to the nature of particle bonding in soil and the role of stabilizing agents, such as the chemical reactions induced by additives. Chemical reactions, including forming pozzolanic or silicate gels in stabilized soils, strengthen particle bonds and increase soil matrix stiffness. This process has the most significant impact on the cohesion parameter, as cohesion is directly related to the degree of resistance of particles to separation.

Overall, the results demonstrate the important role of UPV testing as a non-destructive and reliable method in predicting the mechanical and shear properties of soil.

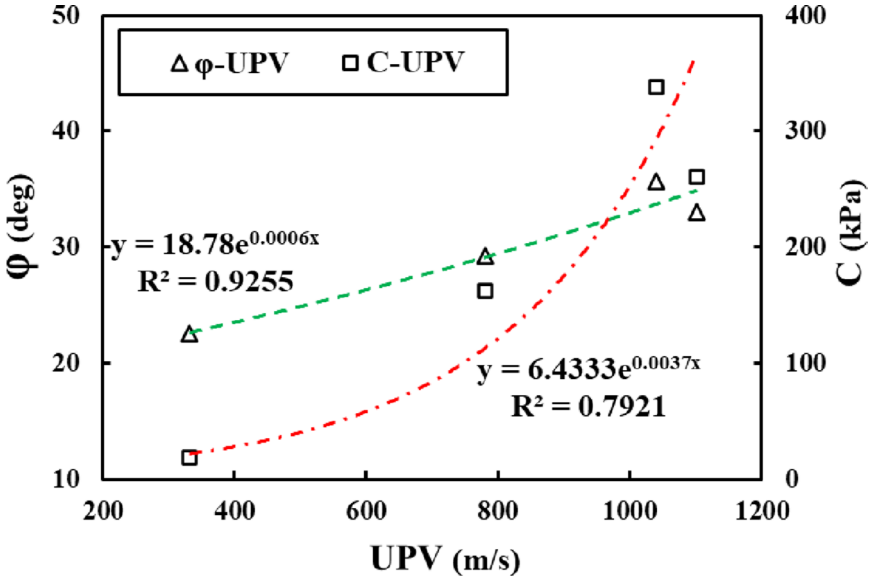

Fig. 23. Relationship between UPV and shear strength parameters, including internal friction angle (φ) and cohesion (c).

Overall, UPV proved to be a sensitive indicator of microstructural improvement, matrix densification, and continuity induced by lime and nano-MgO, while also capturing the slight heterogeneity introduced by PET fibers. The strong correlations between UPV and mechanical parameters confirm its reliability as a non-destructive predictive tool for stabilized soils.

Microstructural analysis

To better understand the mechanisms responsible for the improvement in the mechanical behavior of the stabilized soil, a microstructural analysis was conducted using scanning electron microscopy (SEM). Figure 24 presents the SEM images of the untreated soil and samples stabilized with lime and nano-MgO after 90 days of curing. In the untreated soil sample, the clay particles appear as dispersed plate-like structures with noticeable voids. This loose and porous structure indicates weak bonding between particles, and consequently, the soil has low mechanical strength.

In the lime-stabilized sample, a significant improvement in microstructure is observed. The surface of clay particles is coated with cementitious products formed by pozzolanic reactions between lime and active silica and alumina compounds. These products include C–S–H and C–A–S–H gels that fill the voids and enhance cohesion in the soil matrix by establishing stronger interparticle bonds.

In the stabilized sample with a combination of 10% lime and 2% nano-MgO (the optimal content from the perspective of shear and mechanical parameters), a finer and denser structure is evident compared to other specimens. The presence of nano-MgO particles increases the reactive surface area. It provides nucleation sites, thereby accelerating pozzolanic reactions and promoting the formation of M–S–H gels alongside C–S–H phases. These secondary gels effectively fill almost all the pores, forming a continuous cementitious network between the clay particles. As a result, the observed microstructure changes are consistent with the improvements in the mechanical and shear parameters of the soil, confirming the significant role of the 2% nano-MgO in enhancing the integrity, cohesion, and strength of the stabilized soil.

Figure 25 illustrates the atomic force microscopy (AFM) images of surface topography variations of untreated soil, lime-stabilized soil, and the soil stabilized with a combination of lime and nano-MgO after 90 days of curing. As shown in Fig. 25(a), the untreated soil sample exhibits localized surface elevations ranging from −523 to 871 nm, characterized by sharp and irregular surface roughness features. This morphology reflects the heterogeneous arrangement of clay particles, with limited surface contact between them, resulting in weak interparticle bonding and, consequently, poor mechanical behavior. In contrast, the addition of 10% lime (Fig. 25b) results in a reduced height variation range, from −410 to 380 nm. This reduction is attributed to pozzolanic reactions between lime and active silica and alumina compounds in the soil, leading to the formation of C–S–H and C–A–S–H gels on the particle surfaces. At this stage, the particle surface becomes smoother and more continuous, and initial cementitious bonds are formed between particles.

As depicted in Fig. 25(c), the sample stabilized with the 10% lime + 2% nano-MgO combination exhibits a further reduction in surface roughness, with elevations ranging from −201 to 120 nm. A relatively uniform surface with smooth and dense microstructure is observed. The presence of nano-MgO particles enhances secondary pozzolanic reactions and the formation of additional cementitious phases. These phases significantly improve the structural continuity of the soil matrix by filling the microscopic voids. The progressive reduction in surface roughness from the untreated sample to the lime-stabilized soil and then to the mixture containing lime

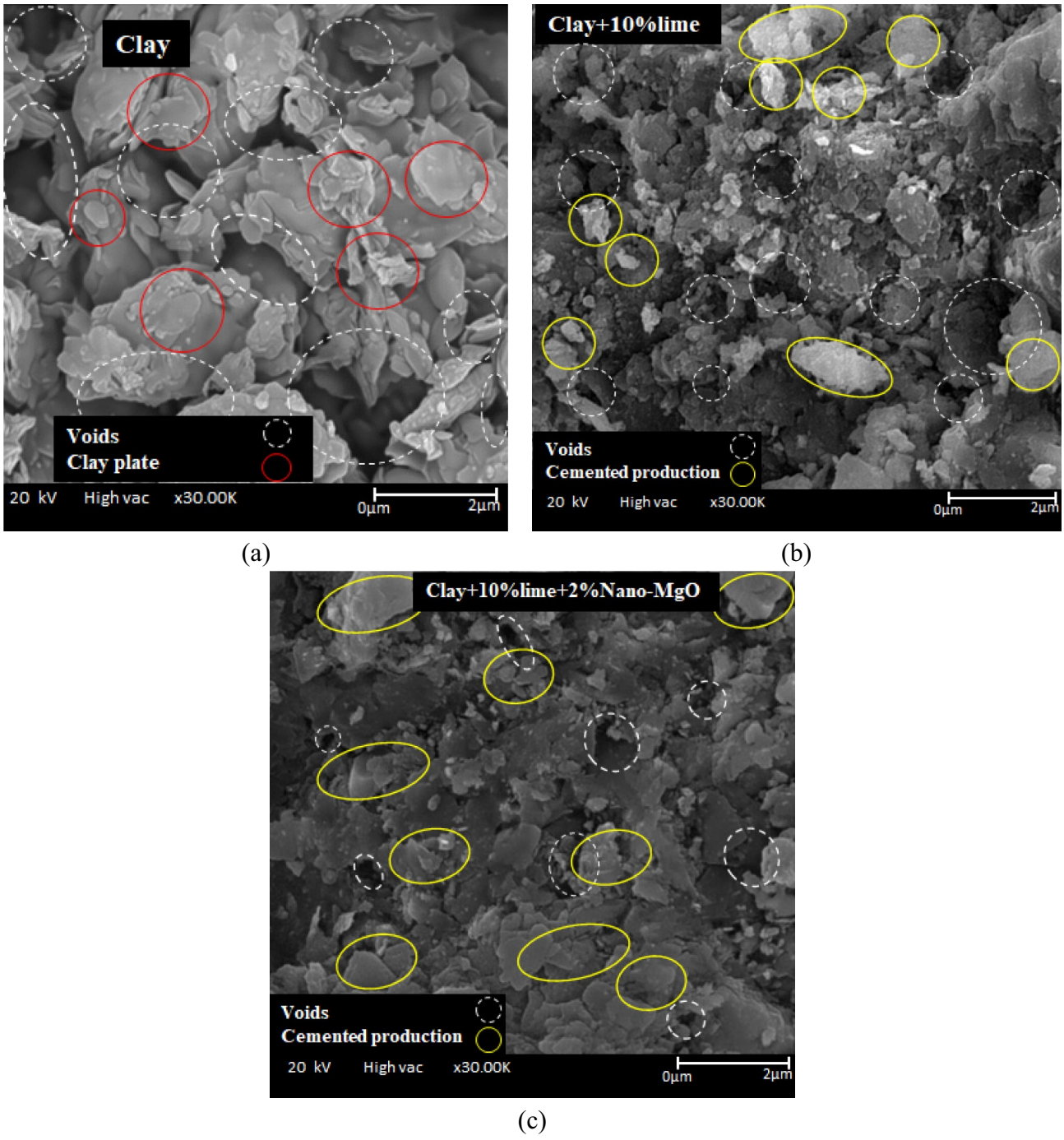

Fig. 24. SEM images of CH clay after 90 days of curing: (**a**) unstabilized clay, (**b**) clay stabilized with 10% lime, and (**c**) clay stabilized with 10% lime and 2% nano-MgO.

and nano-MgO demonstrates a continuous refinement of the microstructure. This improvement corresponds to increased surface adhesion, higher structural densification, and enhanced microscopic integrity.

This nanoscale topographic evolution is fully consistent with the observed improvements in compressive strength and durability of the soil containing the optimum 2% nano-MgO.

The X-ray diffraction (XRD) patterns of the untreated soil, the soil stabilized with lime, and the soil stabilized with lime and nano-MgO are presented in Fig. 26. As shown in Fig. 26(a), the untreated soil exhibits distinct diffraction peaks corresponding to quartz, kaolinite, and montmorillonite. The presence of these minerals is characteristic of highly plastic clays. The distinct quartz peak at $2\theta = 26°$ confirms its crystalline and largely inert nature.

In contrast, kaolinite and montmorillonite are active clay minerals and play a dominant role in the subsequent lime stabilization reactions.

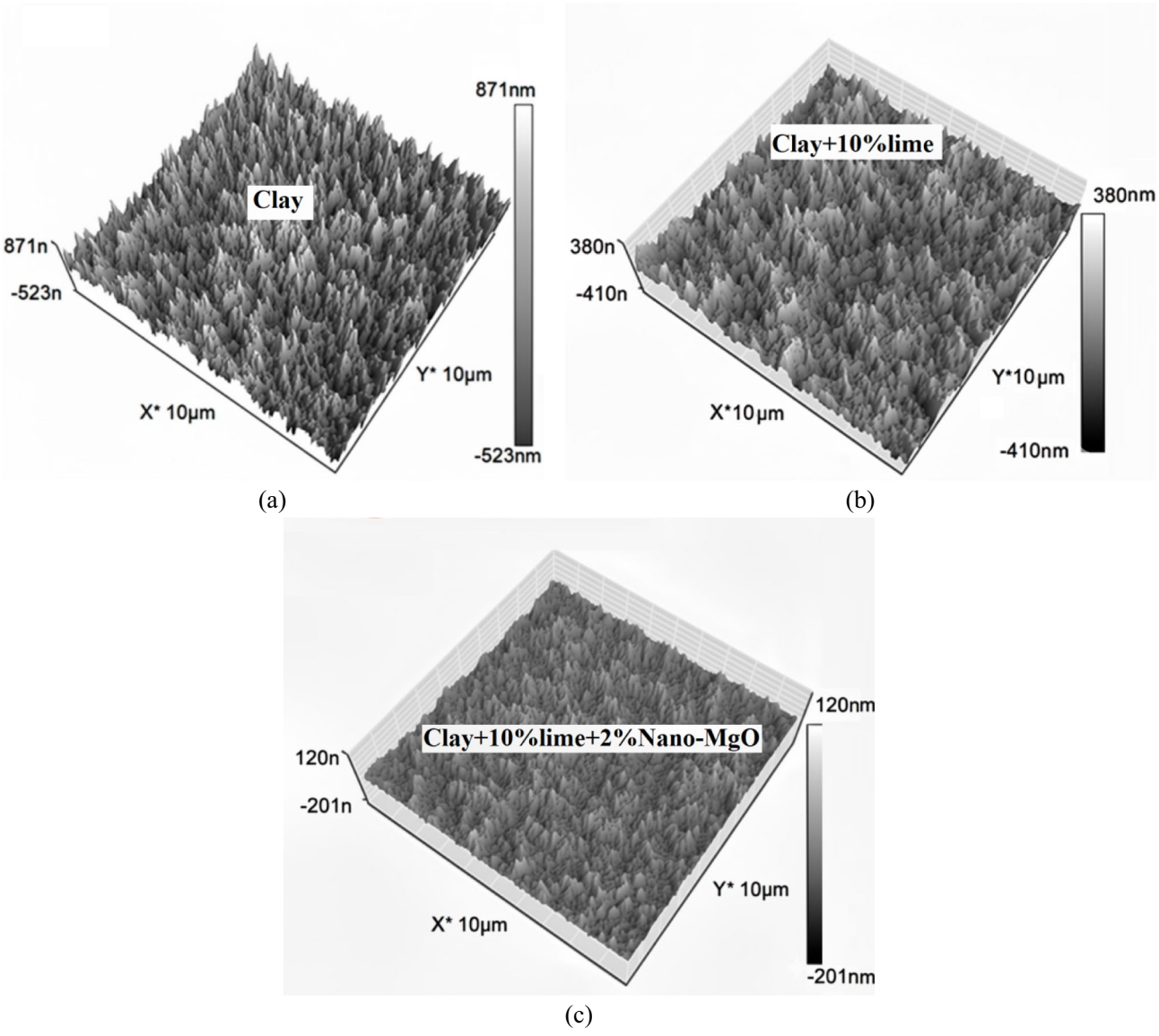

Fig. 25. AFM images of CH clay after 90 days of curing: (**a**) unstabilized clay, (**b**) clay stabilized with 10% lime, and (**c**) clay stabilized with 10% lime and 2% nano-MgO.

In contrast, the lime-stabilized soil (Fig. 26b) exhibits new diffraction peaks in the range of 2θ from 11° to 34°, which are attributed to the formation of C–S–H, C–A–H, and C–A–S–H phases. The decrease of the kaolinite and montmorillonite peaks at this stage indicates their partial consumption in pozzolanic reactions. Additionally, the presence of $Ca(OH)_2$ and $CaCO_3$ peaks suggests that carbonation of free lime has occurred due to its reaction with atmospheric CO_2. These secondary cementitious compounds contribute to interparticle bonding and further enhance the mechanical strength of the soil.

As depicted in Fig. 26(c), the sample stabilized with 10% lime and 2% nano-MgO exhibits considerable changes in the diffraction pattern. The intensity of the peaks related to the C–S–H and C–A–H phases increase, and new phases such as (magnesium silicate hydrate), M–H (magnesium hydroxide), M–C–H (magnesium calcium hydroxide), and Mg–Al–LDH (magnesium–aluminum layered double hydroxides) appeared. These new hydrated phases form as a result of reactions between nano-MgO and the silica and alumina present in the soil. They play a key role in strengthening the soil matrix and reducing microstructural porosity.

The comparison of the three XRD patterns reveals that the addition of lime leads to the formation of primary cementitious phases. In contrast, the presence of nano-MgO accelerates pozzolanic activity and facilitates the formation of more complex and stable hydrated phases, such as M–S–H and Mg–Al–LDH. These microstructural changes are fully consistent with the improvements observed in the mechanical and shear parameters, confirming the beneficial effect of 2% nano-MgO content on enhancing the overall behavior of the soil.

Overall, the microstructural observations obtained from SEM, AFM, and XRD analyses consistently confirm that lime initiates the primary cementitious reactions in the soil.

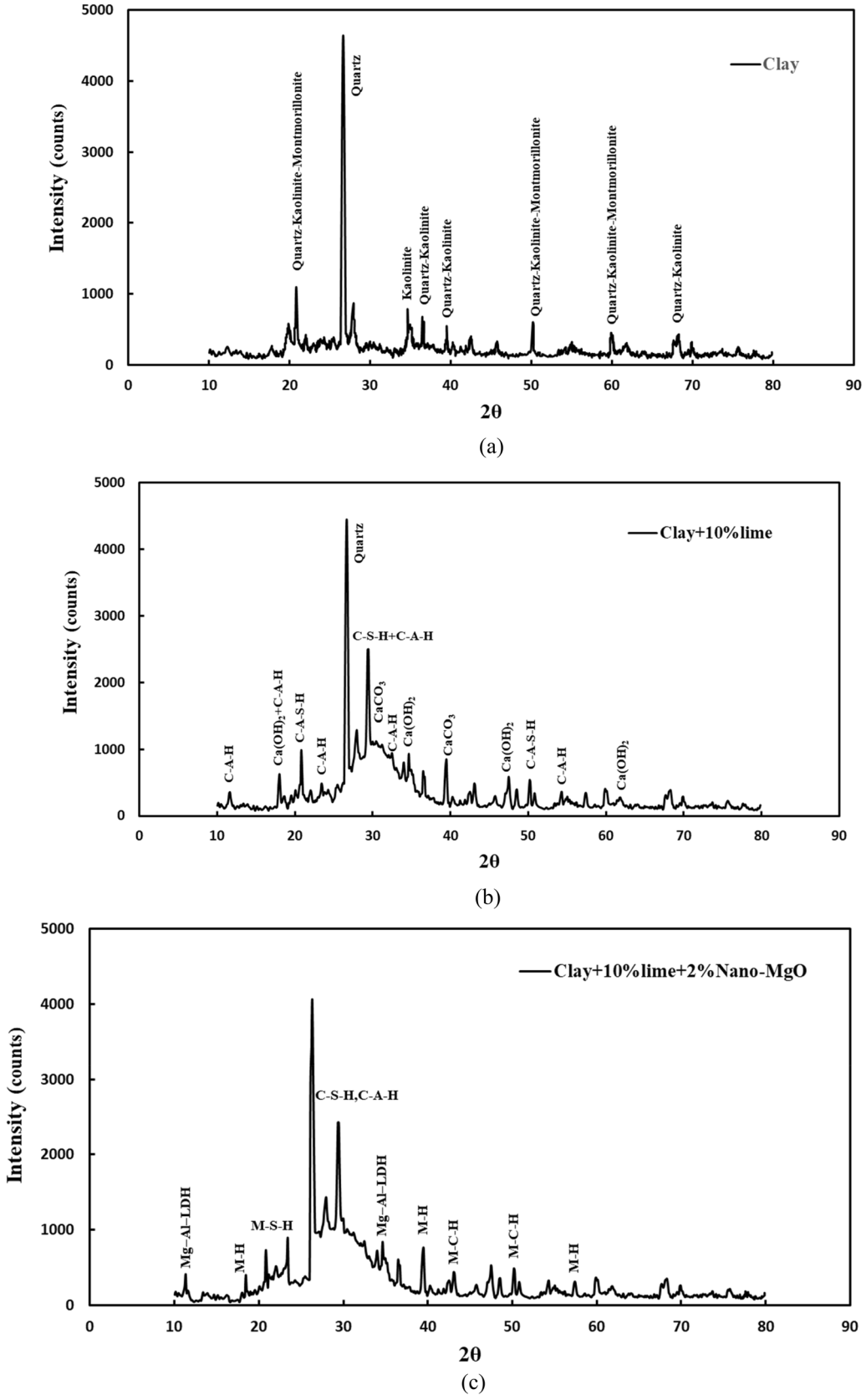

Fig. 26. XRD patterns of CH clay after 90 days of curing: (**a**) natural (unstabilized) clay, (**b**) clay stabilized with 10% lime, and (**c**) clay stabilized with 10% lime and 2% nano-MgO.

Mix type	UCS (kPa)	Strength increase vs. untreated	Additive content (kg/ton soil)	Unit price ($/kg)[1]	Material cost ($/ton soil)
Untreated soil	370.6	–	–	–	0
Lime (10%)	1950.3	+ 426%	100	0.225[1]	22.5
Lime + 2% nano-MgO	2749.6	+ 642%	98 lime + 2 nano-MgO	0.225[1] / 5.0[1]	32.5
[1] Unit prices are based on real market data obtained from Alibaba (2025).					

Table 5. Comparison of strength and material cost at 28 days.

In contrast, nano-MgO accelerates secondary pozzolanic processes and promotes the formation of denser hydration products, such as M–S–H and Mg–Al–LDH, which further improve the soil structure. These combined effects explain the significant improvements observed in strength, stiffness, and shear resistance at the macroscale.

Economic feasibility and cost–performance ratio

To evaluate the practical and economic efficiency of the proposed stabilizer combination, a cost-performance analysis was conducted based on the UCS results at 28 days of curing. Table 5 presents a comparison among the three conditions: unstabilized soil, lime-stabilized soil, and soil stabilized with a combination of lime and nano-MgO.

As shown, the UCS of the unstabilized soil was about 370 kPa. The addition of 10% lime (by dry weight) increased the UCS to approximately 1950 kPa, representing an improvement of more than fourfold (426%) compared to the unstabilized soil. While replacing 2 wt% of lime with nano-MgO increased the UCS to approximately 2750 kPa, the strength became more than six times (642%) higher than that of the unstabilized soil. It was also about 40% higher than the UCS obtained for the soil stabilized with lime alone. This comparison demonstrates that adding a small amount of nano-MgO can effectively enhance the interparticle bonding structure within the soil, resulting in significantly improved mechanical performance.

From an economic perspective, based on market prices, the cost of lime is approximately $0.225 per kilogram, and nano-MgO is in the range of $0.5 to $5 per kilogram; an average value of $ 5 per kilogram was considered for the analysis. Accordingly, the material cost per ton of soil is estimated to be approximately $22.50 for the lime-stabilized sample and $32.50 for the combination of lime and nano-MgO. Therefore, while the material cost has increased by about 45%, the UCS also improves by about 40–50%. Consequently, the cost-to-performance ratio is close to 1:1, indicating that the partial substitution of lime with a small amount of nano-MgO is economically feasible and justified.

Conclusions

This study investigated the stabilization of high-plasticity clayey soils using a combination of lime, Nano-MgO, and PET fibers. The main objective was to improve the mechanical properties of the soil and evaluate the feasibility of non-destructive tests, such as UPV, to predict the mechanical behavior of the soil. Despite the positive findings, this study has limitations, including the lack of durability assessments under extreme environmental conditions and the absence of field-scale behavior investigations, which require further research in the future.

The main findings of this study are as follows:

- Increasing lime content from 0% to 12% led to a reduction in maximum dry density and an increase in optimum moisture content, and the inclusion of nano-MgO intensified this trend.
- The combination of 10% lime and 2% nano-MgO produced the highest mechanical improvement, increasing UCS and ITS by 42.5% and 60%, respectively, after 90 days compared with lime-only samples.
- Nano-MgO contents above 2% resulted in decreases of 26% in UCS and 34% in ITS, indicating the existence of an optimum replacement ratio.
- Adding 0.9% PET fibers to the optimum mixture increased UCS and ITS by 22.5% and 41% after 28 days, while higher fiber contents provided only marginal improvements.
- Extending curing time from 7 to 90 days substantially increased strength, with the optimum mixture showing 195% higher UCS and 140% higher ITS at 90 days.
- Shear strength parameters improved considerably: internal friction angle increased by 58% and cohesion by 47% for the optimum mixture, while PET fibers provided an additional 30% increase in cohesion.
- UPV increased significantly with lime and nano-MgO addition, showing a 158% increase for 10% lime and a further 38% improvement with 2% nano-MgO after 90 days. UPV decreased slightly (4.7%) in fiber-reinforced samples but remained within an acceptable range.
- Strong empirical relationships were established between UPV and mechanical parameters, with R^2 values of 0.91 for UCS, 0.92 for ITS, 0.925 for internal friction angle, and 0.79 for cohesion, confirming UPV as a reliable predictive tool.
- Microstructural analyses (SEM, AFM, XRD) confirmed denser and more uniform fabric in samples containing 10% lime + 2% nano-MgO, consistent with the observed mechanical enhancements.

This study was limited to controlled laboratory conditions, and the performance of stabilized soils was not examined under field-scale loading or varying environmental conditions. Durability aspects, including freeze–

thaw cycles, wetting–drying, moisture fluctuations, and temperature variations, were not evaluated. These limitations may influence the long-term reliability and practical applicability of nano-MgO–stabilized soils.

Future studies should focus on evaluating the field performance of nano-MgO–stabilized soils under real loading and environmental conditions to establish clearer correlations between UPV measurements and mechanical behavior. Since UPV provides a cost-effective and efficient alternative to traditional destructive testing and is particularly valuable for rapid assessment in base and subbase layers, further validation of its applicability in large-scale and in-situ conditions is recommended. Long-term durability assessments involving freeze–thaw cycles, moisture variations, and temperature changes are also necessary to confirm the robustness of this method and to support the development of more sustainable and reliable stabilization strategies.

Data availability

The datasets generated and/or analyzed during the current study are available from the corresponding author on reasonable request.

Received: 5 October 2025; Accepted: 2 February 2026
Published online: 06 February 2026

References

1. Ghazavi, M. & Afrakoti, M. T. P. Experimental study on silty sand contains environmental and friendly construction materials and long-term and short-term behavior: micro and macro study. *Results Eng.* **26**, 104706 (2025a).
2. Ghazavi, M. & Afrakoti, M. T. P. Performance of environmentally friendly biopolymer-natural fiber on post-freeze–thaw behavior on silty sand: Macro- and micro-analysis. *Clean Technol. Environ. Policy*. **27** (9), 4101–4127 (2025b).
3. Ghazavi, M., Taslimi, P. & Afrakoti, M. Effect of natural fiber on durability and strength of problematic soils stabilized with novel Persian gum as an environmentally friendly biopolymer. *J. Mater. Civ. Eng.* **37** (9), 04025289 (2025).
4. Heirani, P. et al. *Eco-friendly Approach To Clay Stabilization: Integrating Carbide lime, Steel slag, and Tire Textile Waste* (Journal of Materials Research and Technology, 2025).
5. Eshghi, P., Azadi, M. & Ahmadi, H. Investigating the Geomechanical behavior and mechanism of clay stabilization with natural zeolite and nano-magnetite under accelerated curing conditions (ACC). *Results Eng.* **24**, 103529 (2024).
6. Ghorbani, A. et al. Effect of selected nanospheres on the mechanical strength of lime-stabilized high-plasticity clay soils. *Adv. Civil Eng.* **2019(1)**, 4257530 (2019).
7. Kutanaei, S. S. & Choobbasti, A. J. Experimental study of combined effects of fibers and Nanosilica on mechanical properties of cemented sand. *J. Mater. Civ. Eng.* **28** (6), 06016001 (2016).
8. Koutenaei, R. Y., Choobbasti, A. J. & Kutanaei, S. S. Triaxial behaviour of a cemented sand reinforced with Kenaf fibres. *Eur. J. Environ. Civil Eng.* **25** (7), 1268–1286 (2021).
9. Kutanaei, S. S. & Choobbasti, A. J. Prediction of combined effects of fibers and cement on the mechanical properties of sand using particle swarm optimization algorithm. *J. Adhes. Sci. Technol.* **29** (6), 487–501 (2015).
10. Raja, M. A. *Application of Nanomaterials and Nanotechnology in the Improvement of Dynamic Properties of Sand and clay. Applications of Nanomaterials in Civil and Environmental Engineering* 125–140 (Towards Sustainable Development and Environment Remediation, 2025).
11. Tavakoli, H. R., Omran, O. L., Shiade, M. F. & Kutanaei, S. S. Prediction of combined effects of fibers and Nanosilica on the mechanical properties of self-compacting concrete using artificial neural network. *Latin Am. J. Solids Struct.* **11**, 1906–1923 (2014).
12. Al Khazaleh, M., Karumanchi, M., Bellum, R. R. & Subramani, A. K. Experimental assessment of geotechnical properties of nano-clay-stabilized soils: advanced sustainable geotechnical solution. *Int. J. Geosynthetics Ground Eng.* **10** (1), 8 (2024).
13. Soltani, A., Moradi, A. & Ahmadi, N. A. Stabilizing clay soils incorporating nanomaterials (through a sustainable development approach). *Environ. Sci. Bioeng.* **8** (1), 65–82 (2019).
14. Bayat, M. *Nanomaterials in Geotechnical Engineering: A Comprehensive Review on Soil Improvement Techniques* (Civil Engineering Infrastructures Journal, 2025).
15. Afrakoti, M. T. P., Choobbasti, A. J., Ghadakpour, M. & Kutanaei, S. S. Investigation of the effect of the coal wastes on the mechanical properties of the cement-treated sandy soil. *Constr. Build. Mater.* **239**, 117848 (2020).
16. Fakhrabadi, A., Ghadakpour, M., Choobbasti, A. J. & Kutanaei, S. S. Influence of the non-woven geotextile (NWG) on the engineering properties of clayey-sand treated with copper slag-based geopolymer. *Constr. Build. Mater.* **306**, 124830 (2021).
17. Fakhrabadi, A., Choobbasti, A. J. & Kutanaei, S. S. Durability evaluation of clayey sandy soil stabilized with copper-slag-based geopolymer under freezing–thawing cycles. *Int. J. Pavement Res. Technol.* **18** (1), 256–273 (2025).
18. Vafaei, A. et al. Effect of barley straw fiber as a reinforcement on the mechanical behavior of Babolsar sand. *Transp. Infrastructure Geotechnology*. **11** (1), 216–235 (2024).
19. Janalizadeh Choobbasti, A., Kutanaei, S., Taslimi, P., Afrakoti, M. & S., & Modeling of compressive strength of cemented sandy soil. *J. Adhes. Sci. Technol.* **33** (8), 791–807 (2019).
20. Kutanaei, S. S., Afrakoti, M. T. P. & Choobbasti, A. J. Effect of coal waste on grain failure of cement-stabilized sand due to compaction. *Arab. J. Geosci.* **14** (12), 1105 (2021).
21. Kutanaei, S. S., Choobbasti, A. J., Afrakoti, M. T. P. & Vafaei, A. Volumetric behavior of cemented sand reinforced with PVA fiber under shear loading. *Transp. Infrastruct. Geotechnol.* **12** (5), 1–26 (2025).
22. Afrakoti, M. T. P., Choobbasti, A. J., Kutanaei, S. S. & Vafaei, A. Effect of hybrid type of fibers on the mechanical properties of stabilized sand with coal waste and cement. *J. Cent. South. Univ.* **31** (11), 4276–4292 (2024).
23. Pouraziz, H., Poursorkhabi, R. V., Fard, M. Y. & Dabiri, R. Experimental investigation of a special chemical additive for improving the geotechnical properties of dispersive clay soils. *Results Eng.* **27**, 107015 (2025).
24. Sharo, A., Bani Baker, M., Tarawneh, D. A., Khasawneh, M. & Ghuzlan, K. Stabilising highly expansive soil by using nano-clay additive. *Int. J. Pavement Eng.* **26** (1), 2460077 (2025).
25. Kheyri, F., Jafary Shalkoohy, A., Eshghi, P. & Ghaderi Niri, H. Synergistic contributions of glass fiber and nano-magnesium oxide to the improvement of physical and mechanical properties of clay soil. *J. Building Pathol. Rehabilitation*. **11** (1), 1–16 (2026).
26. Chen, S., Ni, P., Sun, Z. & Yuan, K. Geotechnical properties and stabilization mechanism of nano-MgO stabilized loess. *Sustainability* **15** (5), 4344 (2023).
27. Wang, W. et al. Mechanical properties and microscopic mechanism of cement-stabilized calcareous sand improved with a nano-MgO additive. *Int. J. Geomech.* **23** (2), 06022040 (2023).
28. Choobbasti, A. J., Samakoosh, M. A. & Kutanaei, S. S. Mechanical properties of soil stabilized with nano calcium carbonate and reinforced with carpet waste fibers. *Constr. Build. Mater.* **211**, 1094–1104 (2019).
29. Yarbaşı, N. & Kalkan, E. The mechanical performance of clayey soils reinforced with waste PET fibers. *Int. J. Earth Sci. Knowl. Appl.* **2** (1), 19–26 (2020).

30. Koohmishi, M. & Palassi, M. Mechanical properties of clayey soil reinforced with PET considering the influence of lime stabilization. *Transp. Geotechnics*. **33**, 100726 (2022).
31. Hasanzadeh, A. & Shooshpasha, I. PET fiber reinforcement efficiency in the mechanical and microstructural characteristics of cemented sand modified with silica fume. *Constr. Build. Mater.* **397**, 132363 (2023).
32. Botero, E., Ossa, A., Sherwell, G. & Ovando-Shelley, E. Stress–strain behavior of a silty soil reinforced with polyethylene terephthalate (PET). *Geotext. Geomembr.* **43** (4), 363–369 (2015).
33. Kannan, G., O'Kelly, B. C. & Sujatha, E. R. Geotechnical investigation of low-plasticity organic soil treated with nano-calcium carbonate. *J. Rock Mech. Geotech. Eng.* **15** (2), 500–509 (2023).
34. Mollaei, M., Jahanian, H. & Azadi, M. Investigation of the effect of nanoclay on the dynamic properties of fine-grained soils. *Indian Geotech. J.* **53** (1), 170–179 (2023).
35. Huang, T., Hou, L., Dai, G., Yang, Z. & Xiao, C. Investigation on strength and flexural behavior of PVA fiber-reinforced and cemented clayey soil. *Buildings* **14** (8), 2433 (2024).
36. Shirvani, R. A. & Noorzad, R. Effectiveness of sludge Ash of wood and paper mill as nontraditional additive for clayey soil treatment. *J. Mater. Civ. Eng.* **31** (10), 04019230 (2019).
37. Noorzad, R. & Motevalian, S. Improvement of clayey soil with lime and industrial sludge. *Geotech. Geol. Eng.* **36**, 2957–2966 (2018).
38. Choobbasti, A. J. & Kutanaei, S. S. Microstructure characteristics of cement-stabilized sandy soil using Nanosilica. *J. Rock Mech. Geotech. Eng.* **9** (5), 981–988 (2017).
39. Tomar, A., Sharma, T. & Singh, S. Strength properties and durability of clay soil treated with mixture of nano silica and polypropylene fiber. *Mater. Today: Proc.* **26**, 3449–3457 (2020).
40. Haeri, S. M. & Valishzadeh, A. Evaluation of using different nanomaterials to stabilize the collapsible loessial soil. *Int. J. Civil Eng.* **19** (5), 583–594 (2021).
41. Mir, B. A. & Reddy, S. H. Mechanical behavior of nano-material (Al_2O_3) stabilized soft soil. *Int. J. Eng.* **34** (3), 636–643 (2021).
42. Cheraghalikhani, M., Niroumand, H. & Balachowski, L. Micro- and nano-bentonite to improve the strength of clayey sand as a nano soil-improvement technique. *Sci. Rep.* **13** (1), 10913 (2023).
43. Gu, J., Cai, X., Wang, Y., Guo, D. & Zeng, W. Evaluating the effect of nano-SiO2 on different types of soils: a multi-scale study. *Int. J. Environ. Res. Public Health*. **19** (24), 16805 (2022).
44. Buazar, F. Impact of biocompatible Nanosilica on green stabilization of subgrade soil. *Sci. Rep.* **9** (1), 15147 (2019).
45. Bagherzadeh Khalkhali, A., Safarzadeh, I. & Rahimi Manbar, H. Investigating the effect of nanoclay additives on the geotechnical properties of clay and silt soil. *J. Civil Eng. Mater. Application*. **3** (2), 65–77 (2019).
46. Abisha, M. R., Anushia, S., Singh, J., Dynisha, J., Lavanya, S. A. & S., & Stabilization of weak clay soil using nanoclay. *Int. J. Ijariie*. **3** (5), 1476–1482 (2017).

Author contributions

Ali Akbar Amiri, Nima Ranjbar Malidarreh (corresponding author), Saman Soleimani Kutanaei, Ali Seyedkazemi, Abdullah Davoudi-Kia contributed to the preparation of all parts of the article.

Declarations

Competing interests

The authors declare no competing interests.

Additional information

Supplementary Information The online version contains supplementary material available at https://doi.org/10.1038/s41598-026-38956-z.

Correspondence and requests for materials should be addressed to N.R.M.

Reprints and permissions information is available at www.nature.com/reprints.

Publisher's note Springer Nature remains neutral with regard to jurisdictional claims in published maps and institutional affiliations.

Open Access This article is licensed under a Creative Commons Attribution-NonCommercial-NoDerivatives 4.0 International License, which permits any non-commercial use, sharing, distribution and reproduction in any medium or format, as long as you give appropriate credit to the original author(s) and the source, provide a link to the Creative Commons licence, and indicate if you modified the licensed material. You do not have permission under this licence to share adapted material derived from this article or parts of it. The images or other third party material in this article are included in the article's Creative Commons licence, unless indicated otherwise in a credit line to the material. If material is not included in the article's Creative Commons licence and your intended use is not permitted by statutory regulation or exceeds the permitted use, you will need to obtain permission directly from the copyright holder. To view a copy of this licence, visit http://creativecommons.org/licenses/by-nc-nd/4.0/.

© The Author(s) 2026